

INFORMATION TO USERS

This manuscript has been reproduced from the microfilm master. UMI films the text directly from the original or copy submitted. Thus, some thesis and dissertation copies are in typewriter face, while others may be from any type of computer printer.

The quality of this reproduction is dependent upon the quality of the copy submitted. Broken or indistinct print, colored or poor quality illustrations and photographs, print bleedthrough, substandard margins, and improper alignment can adversely affect reproduction.

In the unlikely event that the author did not send UMI a complete manuscript and there are missing pages, these will be noted. Also, if unauthorized copyright material had to be removed, a note will indicate the deletion.

Oversize materials (e.g., maps, drawings, charts) are reproduced by sectioning the original, beginning at the upper left-hand corner and continuing from left to right in equal sections with small overlaps. Each original is also photographed in one exposure and is included in reduced form at the back of the book.

Photographs included in the original manuscript have been reproduced xerographically in this copy. Higher quality 6" x 9" black and white photographic prints are available for any photographs or illustrations appearing in this copy for an additional charge. Contact UMI directly to order.

U·M·I

University Microfilms International
A Bell & Howell Information Company
300 North Zeeb Road, Ann Arbor, MI 48106-1346 USA
313/761-4700 800/521-0600

Order Number 9130385

Response of nuclear matter to electromagnetic probes

Wang, Hui-wen, Ph.D.

City University of New York, 1991

U·M·I
300 N. Zeeb Rd.
Ann Arbor, MI 48106

A

**RESPONSE OF NUCLEAR MATTER TO
ELECTROMAGNETIC PROBES**

by

HUI-WEN WANG

A dissertation submitted to the Graduate Faculty in Physics in partial fulfillment of the requirements for the degree of Doctor of Philosophy, The City University of New York

1991

This manuscript has been read and accepted for the Graduate Faculty in Physics in satisfaction of the dissertation requirement for the degree of Doctor of Philosophy.

4-8-91
Date

Carl Shakin
Chair of Examining Committee

4-11-91
Date

Joseph B. Krieger
Executive Officer

Carl M. Shakin

Carl Shakin
Louis S. Celenza

Peter Lesser
Peter Lesser

Peter M. Lesser
Ming-Kung Liou

Ming-Kung Liou
John Gillespie

J. R. Duller
Supervisory Committee

The City University of New York

Abstract

RESPONSE OF NUCLEAR MATTER TO ELECTROMAGNETIC PROBES

by

HUI-WEN WANG

Adviser: Distinguished Professor Carl M. Shakin

We develop methods for the calculation of the hadronic tensor that describes the response of nuclear matter to an electromagnetic probe and study the role of final-state interactions, making use of the theory of Horikawa, Lenz and Mukhopadhyay. Recently, extensive calculations of such final-state interaction effects in quasielastic (e,e') reactions have been performed by Chinn, Picklesimer and Van Orden for finite nuclei. Our nuclear matter calculations reproduce the qualitative features found by those authors, including a significant "quenching" of the longitudinal response, if one uses a relativistic description of the process. While we are able to achieve an improved fit to a body of experimental data for the longitudinal response using this formalism, definitive conclusions cannot be drawn without extending the analysis so that the Ward-Takahashi identity is satisfied. We also find quenching of the transverse response in the region of the quasielastic peak; however, it is unclear as to whether that creates a problem for the theory, since the transverse response is known to have contributions from the excitation

of the delta resonance and various multinucleon processes. We extend the discussion of Bentz, Arima, Hyuga, Shimizu and Yazaki, who considered the role of the Ward-Takahashi identity in the calculation of the electromagnetic response in nuclear matter, to higher values of the momentum transfer. We place particular emphasis on a class of diagrams for which the Ward-Takahashi identity relates the nucleon self-energy to a vertex correction. Consideration of this class of diagrams leads to the definition of an effective one-body model for ejection of a nucleon from the Fermi sea. We provide a systematic diagrammatic analysis for some members of this class of diagrams and indicate how an expansion in powers of the density of the medium may be made. In this manner we exhibit procedures for the evaluation of such corrections.

Acknowledgements

To Professor Carl M. Shakin, my thesis advisor, I wish to express my deepest gratitude for his valuable guidance and constant encouragement throughout this thesis work.

I would also like to express my sincere gratitude to Professor Louis S. Celenza of Brooklyn College of CUNY for many useful discussions and for help given to me during the course of this work.

My thanks also go to Dr. Anthony Pantziris for the help given to me during the course of this work.

I wish to acknowledge with gratitude the Department of Physics of Brooklyn College and the Research Foundation of CUNY for the financial support during the course of this work, and the Brooklyn College Computer Center for allowing me to use their facilities.

CONTENTS

List of Figures	viii
Chapter 1. General Survey	1
1.1 Introduction	1
1.2 Conventions and Notation	8
Chapter 2. Role of Final-State Interactions in the Calculation of the Response Functions of Nuclear Matter	14
2.1 Hadronic Tensor for Relativistic Nuclear Matter	14
2.2 Longitudinal and Transverse Response Functions of Nuclear Matter	24
2.3 Spectral Representation of the Green's Function in Nuclear Matter	28
2.4 Results of Numerical Calculations	34
Chapter 3. Nuclear Matter Ward Identity and the Theory of Final-State Interactions in Inclusive and Exclusive Reactions	40
3.1 Nuclear Matter Ward-Takahashi Identity and Vertex Corrections	40
3.2 A Diagrammatic Analysis of Vertex Corrections in Perturbation Theory	46
3.3 An Estimate of Vertex Corrections Needed in the Presence of Final-State Interactions	55

Chapter 4. One-Body and Many-Body Aspects of the $(e,e'p)$ Reaction: Role of the Ward-Takahashi Identity	57
4.1 Ward-Takahashi Identity and a Density Expansion for the Vertex Corrections in a Nuclear Medium	57
4.2 Evaluation of the Vertex Corrections in a Nuclear Medium	68
4.3 Many-Body Aspects of the Dynamics	75
Chapter 5. Discussion and Conclusions	81
Appendix. The Nucleon Self-Energy in Nuclear Matter	84
References	86

List of Figures

Figure 1.1	Schematic representation of electron scattering from a nucleus in the one-photon-exchange approximation.	1
Figure 1.2	Schematic representation of the cross sections for electron-nucleus and electron-nucleon scattering, as function of the energy transfer ω (for a fixed mementum transfer \vec{q} .)	3
Figure 2.1(a)	Diagram representing the calculation of the virtual (forward) Compton amplitude, $t^{\mu\nu}$, in nuclear matter.	15
(b)	Diagrammatic representation of the calculation of $t^{\mu\nu}$ for an interacting Fermi gas, in the case that some final-state interactions are taken into account.	15
(c)	Diagrammatic representation of the calculation of $\Sigma(p)$ in terms of a nucleon-nucleon reaction matix ¹¹ .	15
Figure 2.2	The values of $a^{(i)}(\epsilon(0)+v, \vec{q})$ are shown for $ \vec{q} = 410$ MeV.	32
Figure 2.3	The values of $a^{(i)}(\epsilon(0)+v, \vec{q})$ are shown for $ \vec{q} = 550$ MeV.	33
Figure 2.4	The longitudinal response function, $R_L(v, \vec{q})$, calculated for ⁴⁰ Ca. [Here $ \vec{q} = 410$ MeV.]	35
Figure 2.5	The transverse response function, $R_T(v, \vec{q})$, calculated for ⁴⁰ Ca. [Here $ \vec{q} = 410$ MeV.]	36
Figure 2.6	The longitudinal response function, $R_L(v, \vec{q})$, calculated for ⁴⁰ Ca. [Here $ \vec{q} = 550$ MeV.]	37
Figure 2.7	The transverse response function, $R_T(v, \vec{q})$, calculated for ⁴⁰ Ca. [Here $ \vec{q} = 550$ MeV.]	38
Figure 3.1	Tadpole diagram representing the lowest-order contribution to the self-energy in nuclear matter.	42
Figure 3.2	Diagrammatic representation of the second-order contributions to the self-energy and to the vertex correction that corresponds to the self-energy $\Sigma^{(2)}(p)$.	47

Figure 3.3(a)	Higher-order corrections to $\Sigma(p)$ calculated in a ladder approximation.	50
(b)	Corrections to the vertex involving an exchange of n bosons, with m exchanges appearing to the left of the photon insertion.	50
Figure 3.4	Schematic representation of the nucleon-nucleon T matrix in the ladder approximation.	53
Figure 3.5(a)	Representation of the self-energy in terms of the nucleon-nucleon T matrix.	54
(b)	The vertex correction, $\Lambda^\mu(p',p)$, corresponding to the self-energy shown in (a).	54
Figure 4.1(a)	Goldstone diagram for the excitation of a particle-hole state by an incident photon (dashed line).	60
(b)	Diagram denoting a wave function renormalization insertion on the hole line.	60
(c)	Goldstone diagrams for some of the vertex corrections, containing two meson lines, that should be considered if final-state interactions are calculated to the same order.	60
Figure 4.2(a)	Many-body Feynman diagrams for the calculation of the self-energy Σ .	62
(b)	The vertex correction, corresponding to the self-energy insertion.	62
(c)	A meson vacuum-polarization diagram.	62
Figure 4.3	Diagrammatic representation of the Green's function of a nucleon in nuclear matter.	64
Figure 4.4(a)	Self-energy insertion and the corresponding vertex correction.	65
(b) and (c)	Self-energy insertions and the corresponding vertex corrections calculated to lowest order in the density of the medium.	65
Figure 4.5	Vertex corrections in which the photon of momentum q couples to a polarization insertion in the meson line.	78
Figure 4.6	Parts of the diagrams of Fig.4.5 are here drawn as photon-meson vertex corrections.	79

Chapter 1

General Survey

1.1 Introduction

One of the basic goals of nuclear physics is to understand the structure of nuclei. Electron scattering offers one of the most important probes of nuclear structure. The process of electron scattering from a nucleus in the one-photon-exchange approximation is shown in Figure 1.1.

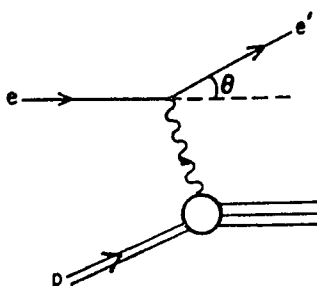


Fig. 1.1

For an unpolarized incident electron beam, the inclusive electron-nucleus cross section is the sum of two terms,

$$\frac{d^2\sigma}{dE'd\Omega} = \sigma_{\text{Mott}} \left[\frac{Q^4}{|\vec{q}|^4} R_L(\vec{q}, \omega) + \left(\frac{1}{2} \frac{Q^2}{|\vec{q}|^2} + \tan^2 \frac{\Theta}{2} \right) R_T(\vec{q}, \omega) \right], \quad (1.1)$$

where σ_{Mott} is the electron scattering cross section for a point charge,

$$\sigma_{\text{Mott}} = \left[\frac{\alpha \cos \frac{\Theta}{2}}{2E \sin^2 \frac{\Theta}{2}} \right]^2. \quad (1.2)$$

$R_L(\vec{q}, \omega)$ and $R_T(\vec{q}, \omega)$ are the longitudinal and transverse response functions and q^μ is the four-momentum of the exchanged (virtual) photon:

$$q^\mu = (\omega, \vec{q}) . \quad (1.3)$$

Neglecting the electron mass, we have

$$Q^2 = -q^2 = 4EE' \sin^2 \frac{\Theta}{2}, \quad (1.4)$$

and

$$\omega = E - E' . \quad (1.5)$$

The response functions, $R_L(\vec{q}, \omega)$ and $R_T(\vec{q}, \omega)$, contain information on the structure of the charge and current distributions in the nucleus.

electron-nucleon scattering as function of the energy transfer ω (for a fixed momentum transfer) are show in Figure 1.2.

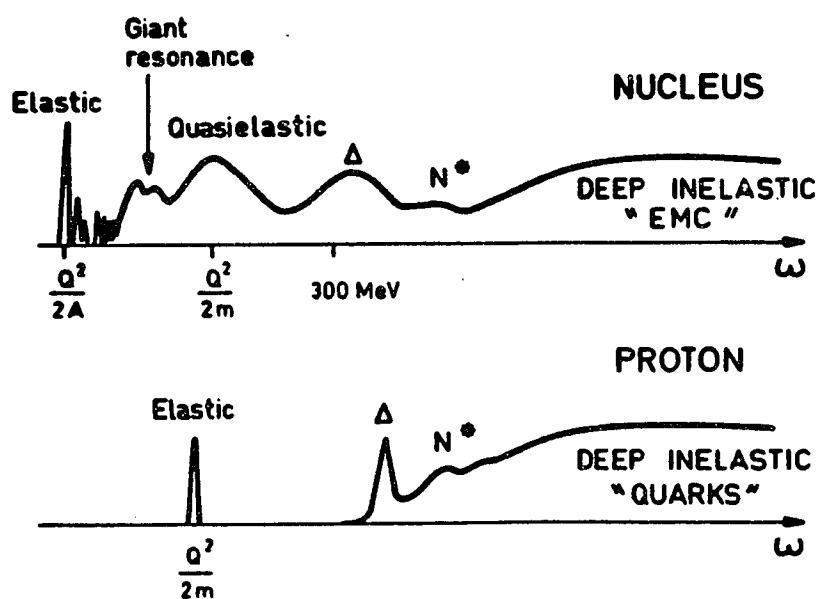


Fig. 1.2

The comparison in Figure 1.2 between electron scattering from a nucleus and from a proton shows a difference arising from the influence of the nuclear medium.

It has become clear in the last decade that the response of a nucleus to an

electromagnetic probe is significantly more complicated than originally thought. For example, it is now believed that the transverse response in (e,e') inclusive reactions contains important multinucleon processes. While the longitudinal response may be free of complications introduced by the presence of multinucleon processes, that response appears to be "quenched" relative to the results of calculations made using a Fermi-gas model or a model which uses the wave functions of finite nuclei. It is hoped, however, that the longitudinal response might be understood in relatively simple terms. A number of mechanisms have been suggested to explain the apparent quenching of the longitudinal response¹; these include relativistic effects^{2,3}, modification of the nucleon properties in the nuclear medium⁴, many-body correlations⁵, final-state interactions^{6,7}, and off-mass-shell effects⁸.

A fully satisfactory theory of (e,e') or $(e,e'p)$ reactions has not been developed thus far. In this connection, we have found the work of Chinn, Picklesimer and Van Orden⁷ to be of interest. The model studied by these authors has a simple interpretation. Basically, one assumes that the nucleon which absorbs the virtual photon in an (e,e') reaction undergoes final-state interactions before leaving the nucleus, the main process being nucleon knockout⁶. The propagation of the struck nucleon may be described by including a complex optical model potential in its Green's function. One might think that such a calculation would just serve to quench the response; however, a careful treatment of the discontinuity structure of the Green's function shows that flux passing into inelastic channels is described properly and that, in principle, sum rules may be preserved⁹. In practise, however, the mechanism described removes strength from the quasielastic

peak and shifts it to higher energies, with the consequence that the integral of the longitudinal response in the region of the quasielastic peak may be significantly reduced from the value it has if one uses a noninteracting Fermi-gas model.

It is of interest to note that the relativistic description of the target leads to different results than the nonrelativistic description when one considers final-state interactions, as in the model explored in Ref. 7. While the inclusion of final-state interactions may explain some features of the experimental data, we stress that calculations of the type made in Ref. 7 and in this work suffer from the defect that current conservation has not been ensured. We have discussed this problem in a recent work¹¹, where we have shown how, in the case of nuclear matter, one can create a formalism which preserves the Ward-Takahashi identity. Therefore, nuclear matter calculations of final-state interactions have the advantage that systematic corrections may be made to the vertex functions. We believe such studies are particularly important, if $(e,e'p)$ reactions are to be used as a tool for the study of nuclear structure. In the case of the electrodisintegration of targets with four or more nucleons, the standard calculation requires that one use a distorted wave for the outgoing nucleon. The potential used to construct the distorted wave is complex; the imaginary part describes the loss of flux from the channel under consideration. We may understand the nature of such approximations by studying the corresponding processes in relativistic nuclear matter. A study of the Ward identity in relativistic nuclear matter was presented in Ref. 12. However, the authors were concerned with small momentum transfer and with the possibility of deriving axial Ward identities. We are here concerned with an extension of the

work of Ref.12 to larger momentum transfer, where the nucleon self-energy becomes complex.

One advantage of nuclear matter studies is that one can clarify the significance of various processes within the context of a diagrammatic analysis. In a first approximation, we may estimate the size of corrections to be expected from a proper treatment of gauge invariance. We have seen in the past that the hadronic response tensor calculated for inclusive scattering from a finite system is well approximated, in the region of the quasielastic peak, by the corresponding tensor calculated in nuclear matter¹¹. Therefore, we suggest that estimates of errors made due to neglect of gauge invariance in the case of nuclear matter may be useful for studies of finite systems.

We have seen some discussion of the role of the Ward-Takahashi identity in constraining the form of the photon-nucleon vertex function. These studies have been made both for many-particle system^{4,10} and for few-body systems¹³. In this work, we discuss the role of the Ward-Takahashi identity in the calculation of the response of nuclear matter to an electromagnetic probe and describe, in greater detail, the form of the vertex corrections that should be included in a theory which exhibits a Ward-Takahashi identity. We also are able to provide some insight into the physical meaning of these vertex corrections. The Ward-Takahashi identity relates the calculation of the self-energy of a particle to the calculation of the vertex correction. In general, there is a very large number of diagrams to be considered in the calculation of the self-energy. However, we are here interested in understanding some aspects of the (e,e') and $(e,e'p)$ reactions. The cross section

for such reactions is usually calculated on the basis of an effective one-body model. One considers a nucleon in a specific orbital and calculates the matrix element of the (free) current operator between the bound orbital and a continuum state. Since the struck nucleon may be removed from the quasi-elastic channel by collisions with nucleons in the residual nucleus, one calculates the continuum wave by solving an equation which contains an optical potential⁷. Care is usually taken to ensure that the optical potential is properly chosen; however, relatively little attention has been given to vertex corrections that are needed if the theory is to exhibit a Ward-Takahashi identity. As we will see, there is a class of diagrams for which the identity may be satisfied. This class of diagrams may be considered as representing an analog of the effective one-body model mentioned above. For the purposes of this work, we can define an effective one-body model as having the following characteristics. The photon may interact with a single nucleon and that nucleon may be traced through the diagram. The nucleon line may be connected to other parts of the diagram by meson propagators¹⁰. The insertions on the nucleon line may be self-energy insertions or vertex corrections. As discussed in our earlier work¹⁰, one may exhibit a Ward-Takahashi identity for the class of diagrams that represent the effective one-body model as described here. In addition, there are diagrams that have an intrinsic many-body aspect and are not related by the Ward-Takahashi identity.

In the next section, we present the conventions and notation used in this work. In Chapter 2 we develop methods for the calculation of the hadronic tensor that describes the response of nuclear matter to an electromagnetic probe and study the role

of final-state interactions in quasi-elastic (e,e') reactions, making use of the theory of Horikawa, Lenz and Mukhopadhyay. As part of our studies, we provided a spectral representation of the Green's function of a nucleon propagating in relativistic nuclear matter. In Chapter 3 we extend the discussion of Bentz, Arima, Hyuga, Shimizu and Yazaki, who considered the role of the Ward-Takahashi identity in the calculation of the electromagnetic response of nuclear matter, to higher values of the momentum transfer. We suggest specific vertex corrections which should provide a more consistent formalism. In Chapter 4 we study a process that is the analog of the $(e,e'p)$ reaction in finite nuclei, making the assumption that the nuclear target may be described as an interacting Fermi gas, in a first approximation. We provide a systematic diagrammatic analysis for some members of the class of diagrams for which the Ward-Takahashi identity relates the nucleon self-energy to a vertex correction, and indicate how an expansion in powers of the density of the medium may be made. In this manner we exhibit procedures for the evaluation of medium corrections. Also we remark upon the many-body aspects of the dynamics. Finally, we present a discussion and some conclusions in Chapter 5.

1.2 Conventions and Notation

In this work we use the conventions and notation specified in the textbooks: Relativistic Quantum Mechanics by J. D. Bjorken and S.D. Drell ¹⁴ and Relativistic

Nuclear Physics: Theory of Structure and Scattering by L. S. Celenza and C. M. Shakin ¹¹.

The metric tensor is

$$g_{\mu\nu} = g^{\mu\nu} = \begin{pmatrix} 1 & 0 & 0 & 0 \\ 0 & -1 & 0 & 0 \\ 0 & 0 & -1 & 0 \\ 0 & 0 & 0 & -1 \end{pmatrix} \quad (1.6)$$

Contravariant coordinate:

$$x^\mu \equiv (x^0, x^1, x^2, x^3) \equiv (x^0, \vec{x}) \quad (1.7)$$

Covariant coordinate:

$$x_\mu \equiv (x_0, x_1, x_2, x_3) \equiv (x_0, -\vec{x}) = g_{\mu\nu}x^\nu \quad (1.8)$$

For any two four-vectors, p and q , the scalar product is

$$p \cdot q = p_\mu q^\mu = p^0 \cdot q^0 - \vec{p} \cdot \vec{q} \quad (1.9)$$

Note that

$$p^2 = p^\mu p_\mu = p_0^2 - \vec{p}^2 \quad (1.10)$$

We may expand the nucleon field operator,

$$\psi(x) = \sum_s \int \frac{d\vec{p}}{(2\pi)^{3/2}} \sqrt{\frac{m}{E(\vec{p})}} \left\{ u(\vec{p},s) e^{-i\vec{p}\cdot x} a_{\vec{p},s} + v(\vec{p},s) e^{i\vec{p}\cdot x} b_{\vec{p},s}^\dagger \right\} ,$$

(1.11)

where

$$u(\vec{p},s) = \sqrt{\frac{E(\vec{p}) + m}{2m}} \begin{pmatrix} \chi_s \\ \frac{\vec{\sigma} \cdot \vec{p}}{E(\vec{p}) + m} \chi_s \end{pmatrix} ,$$

(1.12)

$$v(\vec{p},s) = \sqrt{\frac{E(\vec{p}) + m}{2m}} \begin{pmatrix} \frac{\vec{\sigma} \cdot \vec{p}}{E(\vec{p}) + m} \chi_{-s} \\ \chi_{-s} \end{pmatrix} .$$

(1.13)

Here $u(\vec{p},s)$ and $v(\vec{p},s)$ denote positive-energy and negative-energy spinor solutions of the Dirac equation, respectively; m and \vec{p} are the mass and momentum of the fermion, and χ_s is a Pauli spinor. The $u(\vec{p},s)$ and $v(\vec{p},s)$ satisfy the Dirac equation:

$$\left[\gamma^0 E(\vec{p}) - \vec{\gamma} \cdot \vec{p} - m \right] u(\vec{p},s) = 0 \quad , \quad (1.14)$$

$$\left[\gamma^0 E(\vec{p}) - \vec{\gamma} \cdot \vec{p} + m \right] v(\vec{p},s) = 0 \quad , \quad (1.15)$$

The adjoint spinors

$$\bar{u}(\vec{p},s) = u^\dagger(\vec{p},s) \gamma^0 \quad (1.16)$$

$$\bar{v}(\vec{p},s) = v^\dagger(\vec{p},s) \gamma^0 \quad (1.17)$$

satisfy

$$\bar{u}(\vec{p},s) [\not{p} - m] = 0 \quad (1.18)$$

$$\bar{v}(\vec{p},s) [\not{p} + m] = 0 \quad (1.19)$$

where

$$\gamma^0 = \begin{pmatrix} I & 0 \\ 0 & -I \end{pmatrix}, \quad (1.20)$$

and

$$\vec{\gamma} = \begin{pmatrix} 0 & \vec{\sigma} \\ -\vec{\sigma} & 0 \end{pmatrix}. \quad (1.21)$$

Here, I is a 2×2 unit matrix and $\vec{\sigma}$ denotes the set of 2×2 Pauli spin matrices,

$$\vec{\sigma} = (\sigma_1, \sigma_2, \sigma_3), \quad (1.22)$$

where

$$\sigma_1 = \begin{pmatrix} 0 & 1 \\ 1 & 0 \end{pmatrix} \quad \sigma_2 = \begin{pmatrix} 0 & -i \\ i & 0 \end{pmatrix} \quad \sigma_3 = \begin{pmatrix} 1 & 0 \\ 0 & -1 \end{pmatrix}. \quad (1.23)$$

We also note the following definitions,

$$\sigma^{\mu\nu} = \frac{i}{2} [\gamma^\mu, \gamma^\nu], \quad (1.24)$$

and

$$\gamma^5 = i \gamma^0 \gamma^1 \gamma^2 \gamma^3 = \gamma_5. \quad (1.25)$$

In this representation, the components of $\sigma^{\mu\nu}$ are

$$\sigma^{ij} = \begin{pmatrix} \sigma^k & 0 \\ 0 & \sigma^k \end{pmatrix}, \quad (1.26)$$

with $i, j, k = 1, 2, 3$ in cyclic order and

$$\sigma^{0i} = i \begin{pmatrix} \sigma^k & 0 \\ 0 & \sigma^k \end{pmatrix}. \quad (1.27)$$

Further,

$$\gamma^5 = \begin{pmatrix} 0 & I \\ I & 0 \end{pmatrix}. \quad (1.28)$$

The inner product of γ with an ordinary four-vector is often denoted by

$$\mathcal{K} \equiv \gamma_\mu A^\mu = \gamma^0 A^0 - \vec{\gamma} \cdot \vec{p}, \quad (1.29)$$

$$\not{p} \equiv p^\mu \gamma_\mu = E \gamma^0 - \vec{\gamma} \cdot \vec{p}, \quad (1.30)$$

$$i\not{\not{D}} \equiv p_\mu \gamma^\mu = i\gamma^\mu \frac{\partial}{\partial x^\mu}. \quad (1.31)$$

Chapter 2

Role of Final-State Interactions in the Calculation of the Response Functions of Nuclear Matter

2.1 Hadronic Tensor for Relativistic Nuclear Matter

In Ref.11, the calculation of the hadronic tensor, both for nuclear matter and for finite nuclei, has been discussed using a relativistic formalism. Basically, one may calculate this tensor from the knowledge of the virtual forward Compton amplitude.

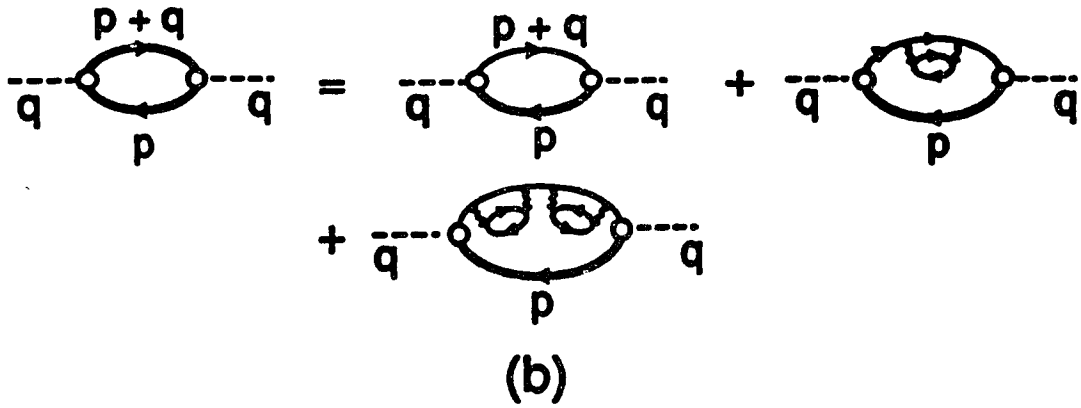
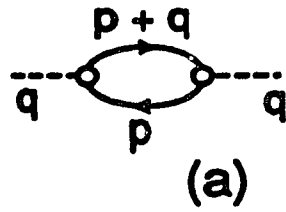
[See Fig. 2.1.]

- Fig.2.1. a) Diagram representing the calculation of the virtual (forward) Compton amplitude, $t^{\mu\nu}$, in nuclear matter, which is described as a noninteracting relativistic Fermi gas. The dashed line denotes a photon of momentum q . The particle line, of momentum $p+q$, represents the free propagator, $G_0(p+q)$. To obtain $W^{\mu\nu}$ from $t^{\mu\nu}$ we need the discontinuity of $G_0(p+q)$, which, in this case, is equivalent to performing the calculation with the particle of momentum $p+q$ on mass shell.
- b) Diagrammatic representation of the calculation of $t^{\mu\nu}$ for an interacting Fermi-gas, in the case that some final-state interactions are taken into account. The heavy line, labeled by $p+q$, represents the Green's function $G(p+q) = [p+q - m_N - \Sigma(p+q)]^{-1}$. A perturbative expansion of that Green's function is shown on the right-hand side, where we have only indicated the nucleon knockout processes which make $\Sigma(p+q)$ complex. All these diagrams contribute to $\text{Disc } G(p+q)$, which is best calculated by using the spectral representation described in Section 2.3.
- c) Diagrammatic representation of the calculation of $\Sigma(p)$ in terms of a nucleon-nucleon reaction matrix¹¹. Values of $A(\vec{p})$, $B(\vec{p})$ and $C(\vec{p})$ obtained in such a calculation¹¹ are used in the work reported here.

In the noninteracting relativistic Fermi-gas model, the Green's function of the struck nucleon, $G(p+q)$, is chosen to be the free Green's function,

$$G_0(p+q) = \frac{1}{p+q - m_N + i\epsilon} . \quad (2.1)$$

The theory explored in Ref. 7 has a nuclear matter analog in which the free Green's function is replaced by the full Green's function



$$\Sigma(p) = \text{[Self-energy loop]} = \text{[Tree-level propagator]} + \text{[Feynman diagram 1]} + \text{[Feynman diagram 2]} + \dots$$

(c)

Fig. 2.1

$$G(p+q) = \frac{1}{\not{p} + \not{q} - m_N - \Sigma(p+q) + i\epsilon} \quad (2.2)$$

[For a nucleon above the Fermi sea, the self-energy, Σ , is complex and we can drop the $i\epsilon$ in Eq. (2.2).]

For simplicity, we will consider the following form of the self-energy

$$\Sigma(p) = A(p) + \gamma^0 B(p) , \quad (2.3)$$

although the analysis is readily extended to treat the more general case where ¹¹

$$\Sigma(p) = A(p) + \gamma^0 B(p) + \frac{\vec{\gamma} \cdot \vec{p}}{m_N} C(p) . \quad (2.4)$$

In our analysis we proceed as follows. We note that $\Sigma(p) = \Sigma(p^0, \vec{p})$ and work in the vicinity of the quasiparticle pole, making use of $\Sigma(\vec{p}) = \Sigma(p^0(\vec{p}), \vec{p})$. Therefore, we have $A(\vec{p}) = A(p^0(\vec{p}), \vec{p})$, etc. [For occupied states we use the notation $\epsilon(\vec{p}) = p^0(\vec{p})$.] Therefore, when we consider $G(p+q)$, the dependence upon $p^0+q^0 = \epsilon(\vec{p})+v$ arises only from the term $p+q$ in Eq. (2.2). The spinor wave functions for an occupied state, in which case $A(\vec{p})$ and $B(\vec{p})$ are real, is denoted as $f(\vec{p}, s)$ and is a solution of ¹¹

$$\left[\vec{\gamma} \cdot \vec{p} + m_N + \Sigma(\vec{p}) \right] f(\vec{p}, s) = \gamma^0 \epsilon(\vec{p}) f(\vec{p}, s) , \quad (2.5)$$

with

$$\varepsilon(\vec{p}) = \text{Re}B(\vec{p}) + \sqrt{\vec{p}^2 + \tilde{m}^2(\vec{p})} \quad , \quad (2.6)$$

and

$$\tilde{m}(\vec{p}) = m_N + \text{Re}A(\vec{p}) \quad . \quad (2.7)$$

If we use the normalization introduced in our previous work ¹¹, we may write

$$f(\vec{p},s) = \left[\frac{E_N(\vec{p})}{m_N} \frac{\tilde{m}(\vec{p})}{\tilde{E}(\vec{p})} \right]^{1/2} u(\vec{p},s,\tilde{m}(\vec{p})) \quad , \quad (2.8)$$

where $E_N(\vec{p}) = [\vec{p}^2 + m_N^2]^{1/2}$ and $\tilde{E}(\vec{p}) = [\vec{p}^2 + \tilde{m}^2(\vec{p})]^{1/2}$. Here $u(\vec{p},s,\tilde{m}(\vec{p}))$ is the spinor, as defined by Bjorken and Drell, with the mass m_N replaced by $\tilde{m}(\vec{p})$. With our choice of normalization, we have

$$f^+(\vec{p},s)f(\vec{p},s) = E_N(\vec{p})/m_N \quad . \quad (2.9)$$

Some off-shell effects are included in the theory by considering a nucleon with four-vector

$$p^\mu = [\varepsilon(\vec{p}), \vec{p}] \quad , \quad (2.10)$$

when $|\vec{p}| < k_F$. We will also use the notation $p_{on}^\mu = [\tilde{\epsilon}(\vec{p}), \vec{p}]$.

Making use of Eq. (2.10), we define the hadronic tensor for scattering from a nucleon in nuclear matter to be

$$w^{\mu\nu} = w_1(-g^{\mu\nu} + \frac{q^\mu q^\nu}{q^2}) + w_2 \frac{\widehat{p}^\mu \widehat{p}^\nu}{m_N^2} \quad , \quad (2.11)$$

where

$$\widehat{p}^\mu = p^\mu - \frac{(p \cdot q)}{q^2} q^\mu \quad . \quad (2.12)$$

In terms of the structure functions w_1 and w_2 , we may define longitudinal and transverse response functions:

$$r_L = \frac{\widehat{p}^2}{m_N^2} \left[-w_1 + \frac{\widehat{p}^2}{m_N^2} w_2 \right] \quad (2.13)$$

and

$$r_T = 2w_1 \quad . \quad (2.14)$$

As noted earlier, $w^{\mu\nu}$ may be obtained from the knowledge of the virtual Compton amplitude. We have

$$w^{\mu\nu}(p,q) = -\frac{1}{\pi} \sum_s \text{Tr} \left[\bar{f}(\vec{p},s) \Gamma^\mu(q) \text{Im} G(p+q) \Gamma^\nu(-q) f(\vec{p},s) \right] \quad (2.15)$$

$$= -\frac{1}{\pi} \left[\frac{\mathbf{E}_N(\vec{p})}{m_N} \frac{\tilde{m}(\vec{p})}{\tilde{\mathbf{E}}(\vec{p})} \right] \frac{1}{2\tilde{m}} \text{Tr} \left[\Gamma^\mu(q) \text{Im} G(p+q) \Gamma^\nu(-q) (\not{p}_{\text{on}} + \tilde{m}) \right] \quad (2.16)$$

where the electromagnetic vertex is

$$\Gamma^\mu(q) = F_1(q^2) \gamma^\mu + i \frac{\sigma^{\mu\nu} q_\nu}{2m_N} F_2(q^2) \quad (2.17)$$

Note that, since $G(p+q)$ is a Dirac matrix, we should more properly write $\text{Im} G(p+q)$ as $\text{Disc} G(p+q)/2$, where $\text{Disc} G(p+q)$ is the discontinuity across the right-hand cut. [See Section 2.3.] We define

$$t^{\mu\nu}(p,q) = \text{Tr} \left[\Gamma^\mu(q) G(p+q) \Gamma^\nu(-q) (\not{p}_{\text{on}} + \tilde{m}) \right] \quad (2.18)$$

and write

$$w^{\mu\nu}(p,q) = -\frac{1}{\pi} \left[\frac{E_N(\vec{p})}{m_N} \frac{\tilde{m}}{E(\vec{p})} \right] \frac{1}{2\tilde{m}} (\text{Im}t^{\mu\nu}) \quad (2.19)$$

At this point, we define three scalar functions, $G^{(i)}(p+q)$, such that

$$G_N(p+q) = G^{(1)}\gamma^0 + G^{(2)}\vec{\gamma} \cdot \frac{(\vec{p}+\vec{q})}{m_N} + G^{(3)} \quad (2.20)$$

To simplify the notation, we introduce a quantity with four components

$$G^\mu(p+q) = (G^{(1)}, -\frac{(\vec{p}+\vec{q})}{m_N} G^{(2)}) \quad (2.21)$$

so that we may write

$$G_N(p+q) = G^\mu(p+q) + G^{(3)}(p+q) \quad (2.22)$$

[Note that the quantity defined in Eq. (2.21) is not a four-vector.]

We find

$$t^{\mu\nu} = 4 \left[g^{\mu\nu}T_1 + (p_{on}^\mu G^\nu + p_{on}^\nu G^\mu)T_2 \right] \quad (2.23)$$

with

$$\begin{aligned}
T_1 = m_N \left\{ G^{(2)} \left[F_1^2 + \frac{q^2}{4m_N^2} F_2^2 \right] - \frac{1}{m_N} F_1 F_2 q \cdot \left[G^{(3)} \frac{p_{on}}{m_N} - G \right] \right. \\
\left. - \left[F_1^2 - \frac{q^2}{4m_N^2} F_2^2 \right] \frac{(p_{on} \cdot G)}{m_N} - \frac{F_2^2}{2m_N^2} \frac{(p_{on} \cdot q)(q \cdot G)}{m_N} \right\}, \quad (2.24)
\end{aligned}$$

and

$$T_2 = F_1^2(q^2) - \frac{q^2}{4m_N^2} F_2^2(q^2), \quad (2.25)$$

where F_1 and F_2 were defined in Eq. (2.17).

We remark that $t^{\mu\nu}$ of Eq. (2.23) does not lead to a tensor $w^{\mu\nu}$ that is of the form given in Eq. (2.11), with $q_\mu w^{\mu\nu} = w^{\mu\nu} q_\nu = 0$. We somewhat arbitrarily remedy that defect by defining

$$t^{\mu\nu} = \left[g^{\mu\lambda} - q^\mu q^\lambda / q^2 \right] T_{\lambda\rho} \left[g^{\rho\nu} - q^\rho q^\nu / q^2 \right], \quad (2.26)$$

$$= 4 \left\{ \left(g^{\mu\nu} - \frac{q^\mu q^\nu}{q^2} \right) T_1 + \left(\hat{p}_{on}^\mu \hat{G}^\nu + \hat{p}_{on}^\nu \hat{G}^\mu \right) T_2 \right\}, \quad (2.27)$$

where, for example,

$$\widehat{G}^\mu = G^\mu - \frac{(G \cdot q)}{q^2} q^\mu , \quad (2.28)$$

etc. Now we have

$$w^{\mu\nu} = -\frac{1}{\pi} \left[\frac{E_N(\vec{p})}{m_N} \frac{\tilde{m}}{\tilde{E}(\vec{p})} \right] \frac{1}{2\tilde{m}} \text{Im} 4 \left\{ \left(g^{\mu\nu} - \frac{q^\mu q^\nu}{q^2} \right) T_1 + \left(\widehat{p}_{\text{on}}^\mu \widehat{G}^\nu + \widehat{p}_{\text{on}}^\nu \widehat{G}^\mu \right) T_2 \right\} . \quad (2.29)$$

We may project w_1 and w_2 from this form by using the relations

$$\widehat{p}^\mu \widehat{p}^\nu w_{\mu\nu} = -\widehat{p}^2 w_1 + \frac{\widehat{p}^4}{m_N^2} w_2 , \quad (2.30)$$

$$\left(g^{\mu\nu} - \frac{q^\mu q^\nu}{q^2} \right) w_{\mu\nu} = -3w_1 + \frac{\widehat{p}^2}{m_N^2} w_2 . \quad (2.31)$$

These equations may be solved for w_1 and w_2 :

$$w_1 = \frac{1}{2} \left[\frac{\widehat{p}^\mu \widehat{p}^\nu}{\widehat{p}^2} w_{\mu\nu} - \left(g^{\mu\nu} - \frac{q^\mu q^\nu}{q^2} \right) w_{\mu\nu} \right] , \quad (2.32)$$

$$w_2 = \frac{m_N^2}{2\hat{p}^2} \left[\frac{3\hat{p}^\mu \hat{p}^\nu}{\hat{p}^2} w_{\mu\nu} - \left(g^{\mu\nu} - \frac{q^\mu q^\nu}{q^2} \right) w_{\mu\nu} \right]. \quad (2.33)$$

Finally, we have,

$$w_1 = -\frac{1}{\pi} \left[\frac{E_N(\hat{p})}{m_N} \frac{\tilde{m}}{\tilde{E}(\hat{p})} \right] \frac{1}{\tilde{m}} \text{Im} \left[-2T_1 + \left(2 \frac{(\hat{p} \cdot \hat{p}_{on})(\hat{p} \cdot \hat{G})}{\hat{p}^2} - 2\hat{p}_{on} \cdot \hat{G} \right) T_2 \right], \quad (2.34)$$

$$w_2 = -\frac{1}{\pi} \left[\frac{E_N(\hat{p})}{m_N} \frac{\tilde{m}}{\tilde{E}(\hat{p})} \right] \frac{1}{\tilde{m}} \frac{m_N^2}{\hat{p}^2} \text{Im} \left[\left(6 \frac{(\hat{p} \cdot \hat{p}_{on})(\hat{p} \cdot \hat{G})}{\hat{p}^2} - 2(\hat{p}_{on} \cdot \hat{G}) \right) T_2 \right]. \quad (2.35)$$

2.2 Longitudinal and Transverse Response Functions of Nuclear Matter

We may now use the definitions of r_L and r_T , given in Eqs. (2.13) and (2.14), and the expressions obtained for w_1 and w_2 to obtain, with $x = Q^2/(2p \cdot q)$,

$$r_L = -\frac{1}{\pi} \frac{\hat{p}^2}{m_N^2} \left[\frac{E_N(\hat{p})}{m_N} \frac{\tilde{m}}{\tilde{E}(\hat{p})} \right] \frac{1}{\tilde{m}} \text{Im} \left[2T_1 + 4 \frac{(\hat{p} \cdot \hat{p}_{on})(\hat{p} \cdot \hat{G})}{\hat{p}^2} T_2 \right], \quad (2.36)$$

and

$$r_T = -\frac{1}{\pi} \frac{\hat{p}^2}{m_N^2} \left[\frac{E_N(\hat{p})}{m_N} \frac{\tilde{m}}{\tilde{E}(\hat{p})} \right] \frac{2}{\tilde{m}} \text{Im} \left[-2T_1 + \left(2 \frac{(\hat{p} \cdot \hat{p}_{on})(\hat{p} \cdot \hat{G})}{\hat{p}^2} - 2(\hat{p}_{on} \cdot \hat{G}) \right) T_2 \right]. \quad (2.37)$$

The hadronic tensor for a nucleus of momentum P_1 and mass M_A may be written

as

$$W^{\mu\nu}(P_1, q) = \left(-g^{\mu\nu} + \frac{q^\mu q^\nu}{q^2} \right) W_1 + \frac{\hat{P}_1^\mu \hat{P}_1^\nu}{M_A^2} W_2. \quad (2.38)$$

From that quantity we obtain averaged values of longitudinal and transverse response functions for a nucleon in nuclear matter:

$$\begin{aligned}
\bar{r}_L(x_i, Q^2) &= \frac{1}{2\Omega} \int \frac{d\vec{p}}{(2\pi)^3} \frac{m_N}{E_N(\vec{p})} \Theta(k_F - |\vec{p}|) \Theta(|\vec{p} + \vec{q}| - k_F) \\
&\times \left\{ r_L \left(\frac{E_N(\vec{p})}{m_N} + \frac{Q^2}{4m_N^2 x_i} \right)^2 / \left(1 + \frac{Q^2}{4m_N^2} \right)^2 \right. \\
&\quad \left. + \frac{r_T}{2} \left[\left(\frac{E_N(\vec{p})}{m_N} + \frac{Q^2}{4m_N^2 x_i} \right) / \left(1 + \frac{Q^2}{4m_N^2} \right) - \left(1 + \frac{Q^2}{4m_N^2 x_i^2} \right) \right] \right\}
\end{aligned} \tag{2.39}$$

$$\begin{aligned}
\bar{r}_T(x_i, Q^2) &= \frac{1}{2\Omega} \int \frac{d\vec{p}}{(2\pi)^3} \frac{m_N}{E_N(\vec{p})} \Theta(k_F - |\vec{p}|) \Theta(|\vec{p} + \vec{q}| - k_F) \\
&\times \left\{ \frac{r_T}{2} \left[1 + \frac{\left(\frac{E_N(\vec{p})}{m_N} + \frac{Q^2}{4m_N^2 x_i} \right)^2}{\left(1 + \frac{Q^2}{4m_N^2} \right) \left(1 + \frac{Q^2}{4m_N^2 x_i^2} \right)} \right] \right. \\
&\quad \left. + \frac{r_L}{\left(1 + \frac{Q^2}{4m_N^2} \right)} \left[\frac{\left(\frac{E_N(\vec{p})}{m_N} + \frac{Q^2}{4m_N^2 x_i} \right)^2}{\left(1 + \frac{Q^2}{4m_N^2} \right) \left(1 + \frac{Q^2}{4m_N^2 x_i^2} \right)} - 1 \right] \right\} .
\end{aligned} \tag{2.40}$$

where

$$\Omega = \int \frac{d\vec{p}}{(2\pi)^3} \Theta(k_F - |\vec{p}|) \quad (2.41)$$

and

$$x_t = \frac{Q^2}{2m_N v} \quad (2.42)$$

[Note that only for a nucleon at rest in the laboratory frame would $x = x_t$.]

It may be seen that the following approximation is quite accurate:

$$\bar{r}_L(x_t, Q^2) \approx \frac{1}{2\Omega} \int \frac{d\vec{p}}{(2\pi)^3} \frac{m_N}{E_N(\vec{p})} \Theta(k_F - |\vec{p}|) \Theta(|\vec{p} + \vec{q}| - k_F) r_L \quad (2.43)$$

and

$$\bar{r}_T(x_t, Q^2) \approx \frac{1}{2\Omega} \int \frac{d\vec{p}}{(2\pi)^3} \frac{m_N}{E_N(\vec{p})} \Theta(k_F - |\vec{p}|) \Theta(|\vec{p} + \vec{q}| - k_F) r_T \quad (2.44)$$

Note that the factor of (1/2) which appears on the right-hand side effectively

replaces r_L and r_T by their spin-averaged values, $r_L/2$ and $r_T/2$. Approximate response functions for finite nuclei may be obtained by including factors of N and Z , the numbers of neutrons and protons:

$$R_L(x_i, Q^2) = Z \bar{r}_L^{(p)}(x_i, Q^2) + N \bar{r}_L^{(n)}(x_i, Q^2) , \quad (2.45)$$

and

$$R_T(x_i, Q^2) = Z \bar{r}_T^{(p)}(x_i, Q^2) + N \bar{r}_T^{(n)}(x_i, Q^2) . \quad (2.46)$$

The calculation of w_1 and w_2 , or r_L and r_T , requires a knowledge of the discontinuity of the Green's function, $G(p+q)$, across the right-hand cut. [This discontinuity may be obtained from the knowledge of the imaginary parts of the scalar functions $G^{(i)}(p+q)$.] We discuss a spectral representation of the Green's function in the next section.

2.3 Spectral Representation of the Green's Function in Nuclear Matter

Consider the general form taken by $\Sigma(\vec{p})$ in nuclear matter

$$\Sigma(\vec{p}) = A(\vec{p}) + B(\vec{p})\gamma^0 + \frac{\vec{\gamma} \cdot \vec{p}}{m_N} C(\vec{p}) . \quad (2.47)$$

It is useful to write this $\Sigma(\vec{p})$ as

$$\Sigma(\vec{p}) = A + \mathcal{B} , \quad (2.48)$$

where we have defined a four-component object

$$B_\mu = [B(\vec{p}), - C(\vec{p})\vec{p}/m_N] \quad (2.49)$$

for notational convenience. We have

$$G(p) = [\not{p} - m_N - \Sigma]^{-1} \quad (2.50)$$

$$= [\not{p} - \mathcal{B} - m_N - A]^{-1} \quad (2.51)$$

$$= G^{(1)}\gamma^0 + G^{(2)}\frac{\vec{\gamma} \cdot \vec{p}}{m_N} + G^{(3)} \quad (2.52)$$

$$= \mathcal{G} + G^{(3)} . \quad (2.53)$$

We may construct $G(p)$ from the knowledge of A , B and C . These potentials were calculated for nuclear matter and some values of these quantities were presented in

Ref. 11. Analytical approximations which represent these potentials are given in the Appendix.

In order to calculate the discontinuity of $G(p+q)$ needed for our calculation, it is useful to construct a spectral representation. We define

$$G(p) = \frac{1}{\pi} \int dp_0 \frac{[a^{(1)}(p_0, \vec{p})\gamma^0 + a^{(2)}(p_0, \vec{p})\vec{\gamma} \cdot \vec{p}/m_N + a^{(3)}(p_0, \vec{p})]}{p_0 - p_0 + i\eta} . \quad (2.54)$$

From this we have

$$\frac{1}{2} \text{Disc } G(p) = - [a^{(1)}(p^0, \vec{p})\gamma^0 + a^{(2)}(p^0, \vec{p})\vec{\gamma} \cdot \vec{p}/m_N + a^{(3)}(p^0, \vec{p})] \quad (2.55)$$

We then note that $a^{(i)}(p+q) = -\text{Im } G^{(i)}(p+q)$, with $i = 1,2,3$. Therefore we have

$$\frac{1}{2} \text{Disc } G(p+q) = \text{Im}G^{(1)}(p+q)\gamma^0 + \text{Im}G^{(2)}(p+q)\vec{\gamma} \cdot \vec{p}/m_N + \text{Im}G^{(3)}(p+q) , \quad (2.56)$$

which can be taken as the definition of the expression $\text{Im } G(p+q)$ used in Eq. (2.16), etc.

Recall that v was the value of q^0 in the laboratory frame. Then $p+q = (\epsilon(\vec{p})+v, \vec{p}+\vec{q})$, which for a nucleon at rest is $p+q = (\epsilon(0)+v, \vec{q})$. In Figs 2.2 and 2.3 we exhibit values of $a^{(i)}(\epsilon(0)+v, \vec{q})$, for $|\vec{q}| = 410\text{MeV}$ and $|\vec{q}| = 550\text{MeV}$,

These values were obtained upon including the terms $A(\vec{p})$, $B(\vec{p})$ and $C(\vec{p})$ in $\Sigma(\vec{p})$. [Only small changes appear in the $a^{(i)}$, if we neglect $C(\vec{p})$ entirely.] Note that, in the absence of final-state interactions, the $a^{(i)}$ would appear as delta functions. The position of the delta functions for the case $\vec{p} = 0$ would be at $v = [m_N^2 + \vec{q}^2]^{1/2} - m_N$. (The position of the peak in Figs. 2.2 and 2.3 is shifted from that value due to the presence of the self energy, $\Sigma(0)$, in the initial state and $\Sigma(\vec{q})$ in the final state.

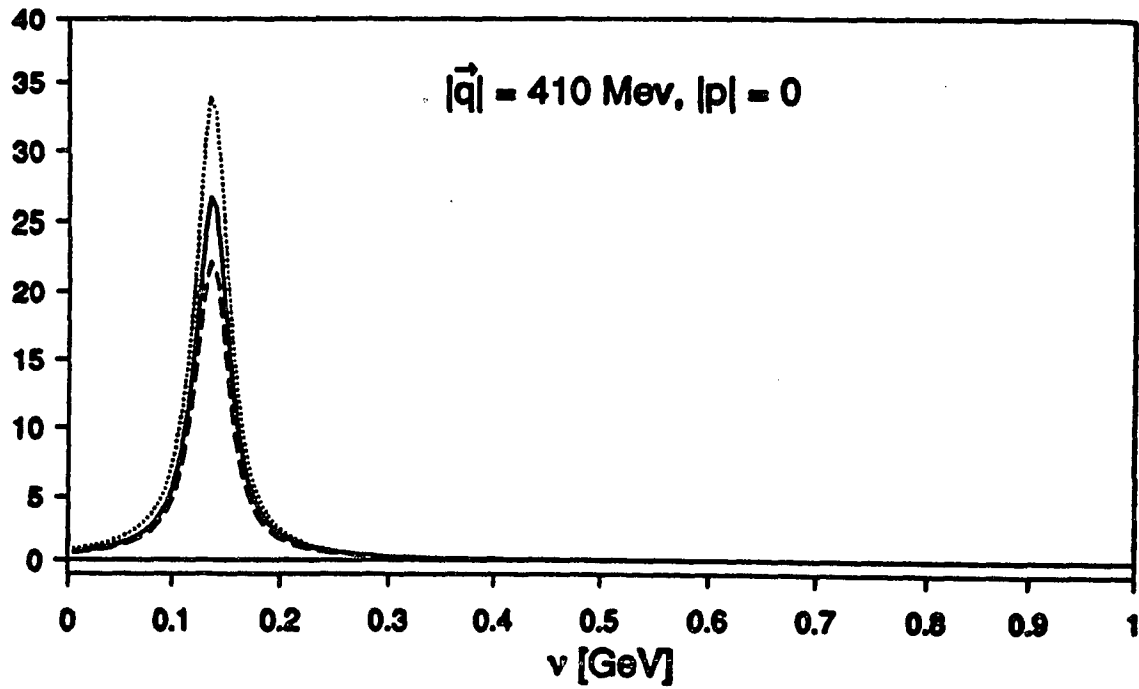


Fig. 2.2

The values of $a^{(i)}(\epsilon(0)+v,\vec{q})$ are shown for $|\vec{q}| = 410 \text{ MeV}$. Here the terms $A(\vec{p})$, $B(\vec{p})$ and $C(\vec{p})$ were included in $\Sigma(\vec{p})$ and were taken from Ref.11. [See Appendix.] The solid line represents $a^{(1)}$, the dotted line denotes $-a^{(2)}$ and the dashed line is $a^{(3)}$.

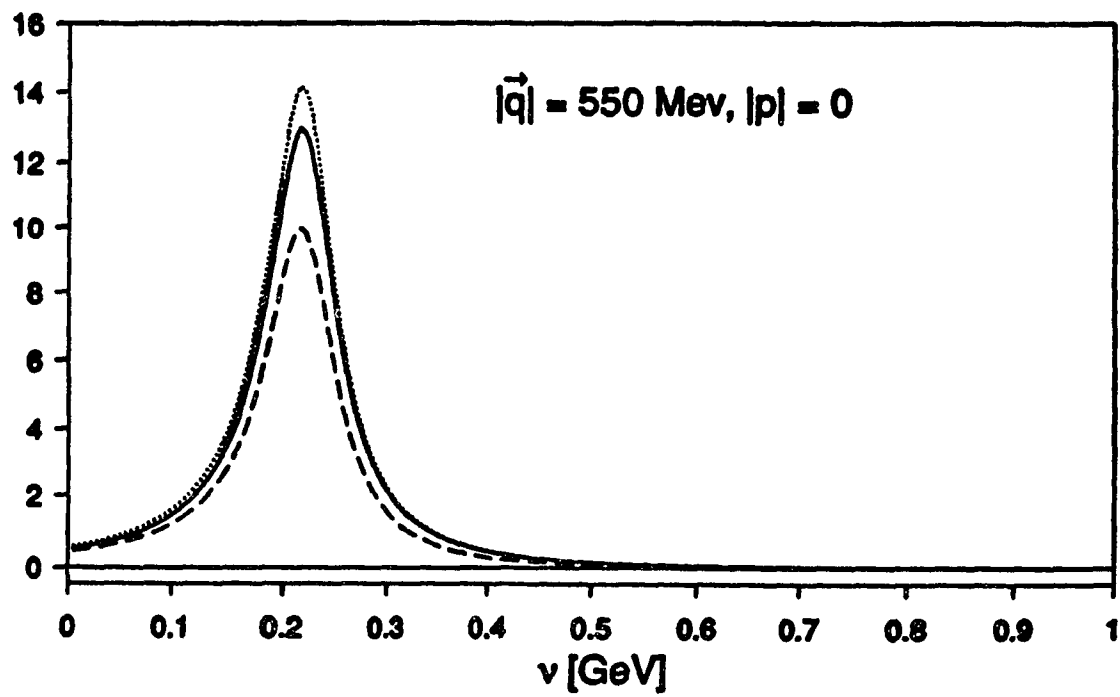


Fig. 2.3

Same caption as Fig.2.2, except that $|\vec{q}| = 550 \text{ MeV}$.

2.4 Results of Numerical Calculations

As a check on the numerical procedure we used the same computer code to calculate the response functions for finite values of Σ and for the Fermi-gas model. In the latter case we put the real parts of A, B and C equal to zero, as well as the imaginary parts of B and C. The imaginary part of A was put equal to a small quantity, $\eta \approx 10$ MeV. That approximation reproduced the results obtained for the free Fermi-gas model in previous calculations, except for some small tails on the distribution which would vanish if the calculation were done for $\eta \rightarrow 0$. Once satisfactory results were obtained for the free Fermi-gas model, we used the values of $A(\vec{p})$, $B(\vec{p})$ and $C(\vec{p})$ given in the Appendix to perform the calculations described in Sections 2.1 and 2.2. Using the formalism outlined there, we calculated the longitudinal and transverse response functions, $R_L(v, |\vec{q}|)$ and $R_T(v, |\vec{q}|)$, for ^{40}Ca at $|\vec{q}| = 410$ MeV and 550 MeV. The results obtained are exhibited in Figs. 2.4 - 2.7. Figures 2.4 and 2.5 show the results for $|\vec{q}| = 410$ MeV, while Figs. 2.6 and 2.7 exhibit the results at $|\vec{q}| = 550$ MeV. As may be seen from the figures, we find quenching for both the transverse and longitudinal response functions. In the case of the longitudinal response, there is a significant improvement seen when comparing theory and experiment. We also note that the results obtained here are similar to those exhibited in Ref. 7 in the case that Dirac phenomenology was used for the description of the final-state interaction. (We remark that somewhat different behavior was observed in Ref. 7, depending upon whether a

relativistic or nonrelativistic formalism was used.) To the extent that the calculation is meaningful, it may be concluded that the agreement with the data is better in the case of the relativistic analysis, since, in that case, the longitudinal response is quenched to a greater degree than the transverse response.

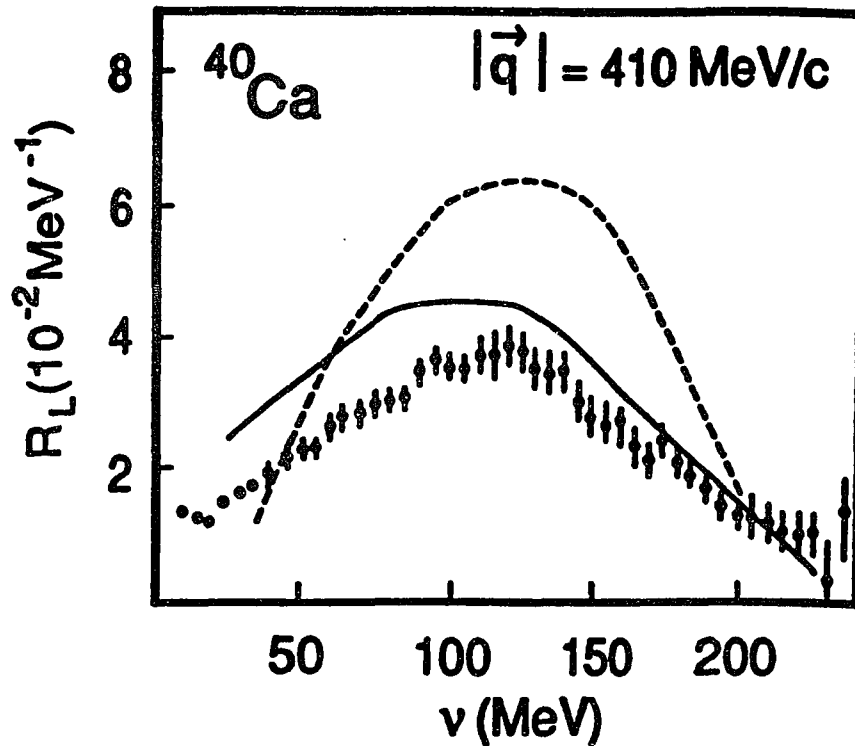


Fig. 2.4

The dashed curve shows the longitudinal response function, $R_L(\nu, |\vec{q}|)$, calculated for a noninteracting Fermi gas. Also shown is experimental data for ^{40}Ca . [Here $|\vec{q}| = 410 \text{ MeV}$.] The theoretical curve is shifted upward in energy by 30 MeV to take into account differences of binding of the occupied and continuum orbitals. We have put $\rho = 0.60\rho_{\text{NM}}$, where ρ_{NM} is the density of nuclear matter [$\rho_{\text{NM}} = 0.17\text{fm}^{-3}$]. The solid line shows the result obtained if final-state interactions are included using the methods described in the text.

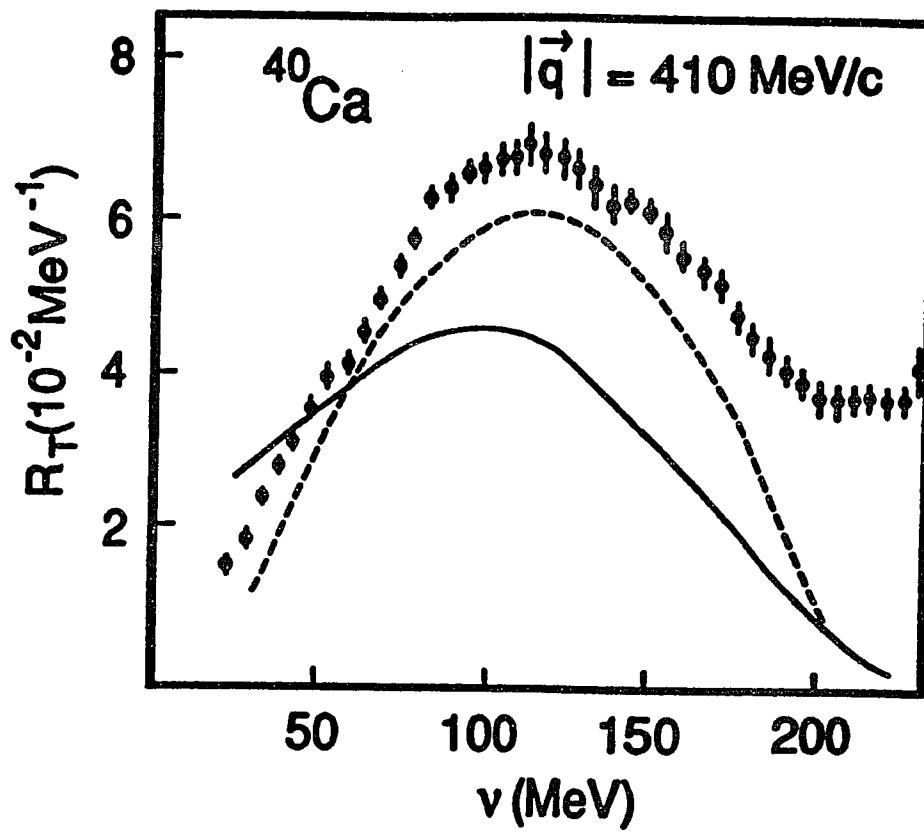


Fig. 2.5

Same caption as Fig. 2.4, except that the transverse response is shown.

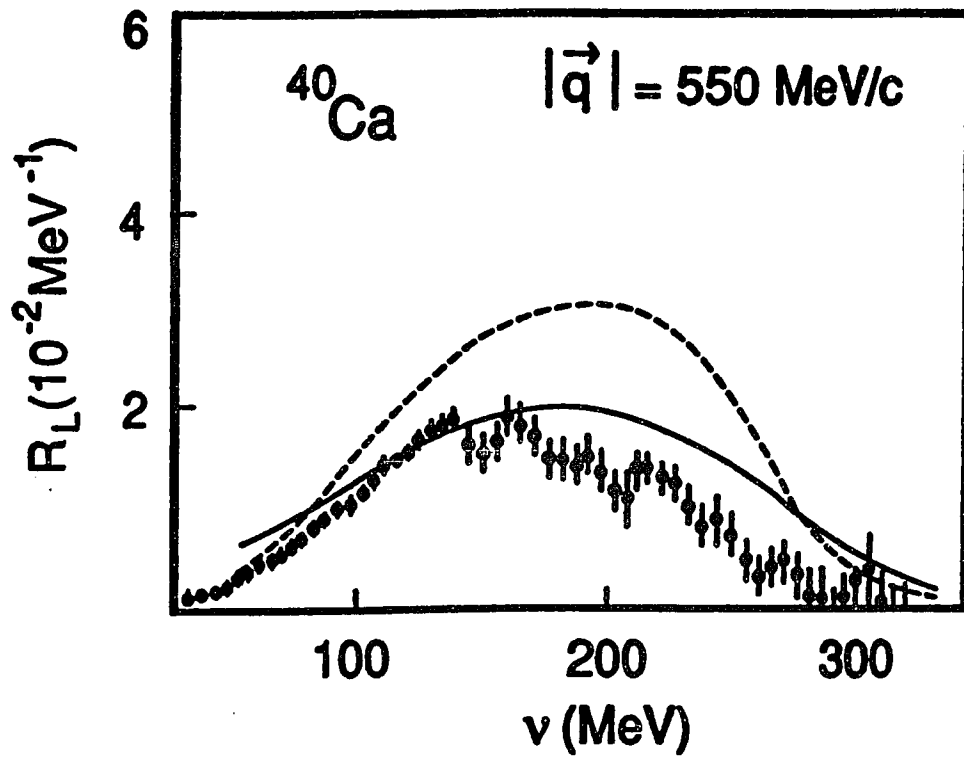


Fig.2.6

Same caption as Fig.2.4, except that $|\vec{q}| = 550 \text{ MeV}$.

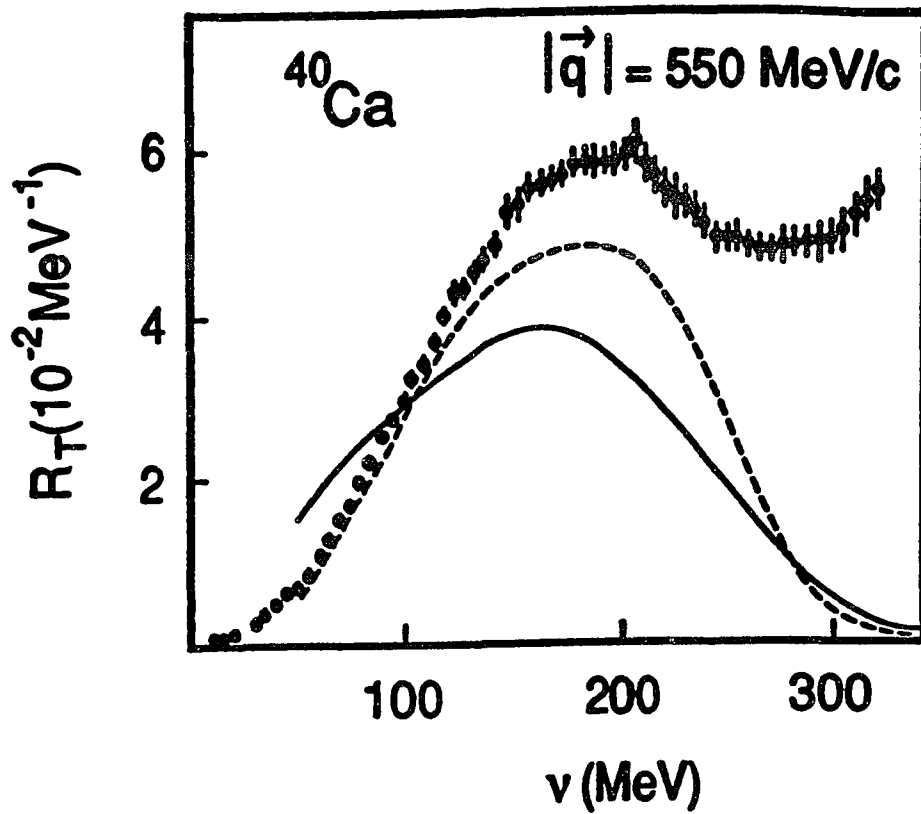


Fig. 2.7

Same caption as Fig. 2.4, except that the transverse response is shown for $|\vec{q}| = 550 \text{ MeV}$.

Chapter 3

Nuclear Matter Ward Identity and the Theory of Final-State Interactions in Inclusive and Exclusive Reactions

3.1 Nuclear Matter Ward-Takahashi Identity and Vertex Corrections

In Chapter 2 we studied the role of final-state interactions which may be included in the calculation of (e,e') inclusive or $(e,e'p)$ reactions, for example. The standard method for performing these calculations may be seen to be inconsistent. A consistent theory should include the vertex corrections that are required in an analysis which preserves the Ward-Takahashi identity.

The Green's function of a nucleon in the relativistic nuclear matter is

$$G(p) = \frac{1}{\not{p} - m_N - \Sigma(p)} \quad (3.1)$$

and this Green's function may be written as

$$G(p) = \frac{m}{E(p)} \sum_s \left[\frac{f(p,s)\bar{f}(p,s)}{p^0 - \epsilon(p^0, \vec{p}) + i\eta} \Theta(|\vec{p}| - k_F) + \frac{f(p,s)\bar{f}(p,s)}{p^0 - \epsilon(p^0, \vec{p}) - i\eta} \Theta(k_F - |\vec{p}|) \right] \quad (3.2)$$

if $\gamma^0 \Sigma$ is Hermitian. Here we have dropped the negative-energy states, in keeping with the approximations used in relativistic Brueckner-Hartree-Fock theory¹¹. We may define spinors, $f(\vec{p}, s)$, by evaluating the spinors $f(p, s) = f(p^0, \vec{p}, s)$ at the quasi-particle pole,

$$f(\vec{p}, s) = f(p^0, \vec{p}, s) |_{p^0 = \epsilon(\vec{p})} . \quad (3.3)$$

[Note that, if A and B are independent of p^0 , the form given in Eq. (3.1) simplifies.]

For the purposes of this discussion, we will use the most elementary form of the Walecka model³, neglecting correlations and exchange; however, the formalism may be generalized to include more complex models.

In Fig. 3.1 we show the leading approximation for the self-energy,

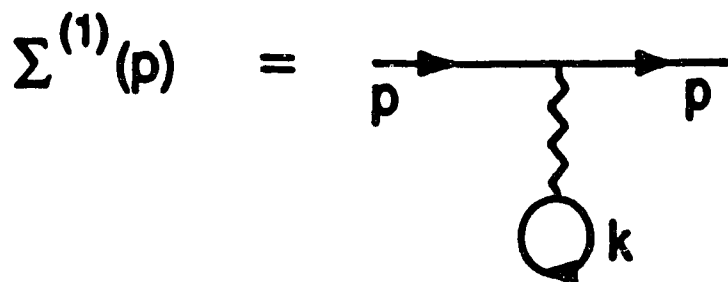


Fig.3.1

Tadpole diagram representing the lowest-order contribution to the self-energy in nuclear matter. Here k labels an occupied state.

This approximation leads to constant values for the scalar and vector potentials ¹¹ :

$$\Sigma^{(1)} = A^{(1)} + \gamma^0 B^{(1)} \quad (3.4)$$

$$= -\frac{g_\sigma^2 \rho_S}{m_\sigma^2} + \frac{g_\omega^2 \rho_B}{m_\omega^2} \gamma^0 \quad (3.5)$$

In Eq. (3.4), ρ_S is the scalar density and ρ_B is the baryon density of nuclear matter; g_σ and m_σ are the coupling constant and mass of the sigma meson, etc. Using this elementary approximation, we can calculate matrix elements of the current between the

states $f(\vec{p},s)$ and $f(\vec{p}+\vec{q},s)$,

$$(\vec{p}+\vec{q},s' | J^\mu(0) | \vec{p},s) = \bar{f}(\vec{p}+\vec{q},s') \left[\gamma^\mu F_1(q^2) + i \frac{\sigma^{\mu\nu}}{2m_N} q_\nu F_2(q^2) \right] f(\vec{p},s) \quad (3.6)$$

and one readily sees that the current is conserved, $(\vec{p}+\vec{q},s' | q^\mu J_\mu(0) | \vec{p},s) = 0$. In the case of conserved currents, the hadronic response tensor may be obtained in the standard form for a nuclear target of momentum P ,

$$W^{\mu\nu}(q,P) = \left(-g^{\mu\nu} + \frac{q^\mu q^\nu}{q^2} \right) W_1(q,P) + \frac{\hat{P}^\mu \hat{P}^\nu}{M_A^2} W_2(q,P) \quad (3.7)$$

where W_1 and W_2 are structure functions for the target of mass M_A and $\hat{P}^\mu = P^\mu - (P \cdot q)q^\mu/q^2$.

At this point we may consider the modification of the vertex required to maintain current conservation in the case Σ is not constant. We consider the density-dependent vertex correction for protons, $\Lambda^\mu(p',p)$. We have, on quite general grounds,

$$q^\mu \Lambda_\mu(p',p) = - (\Sigma(p') - \Sigma(p)) \quad (3.8)$$

as discussed in Ref. 12. Let us now separate $\Lambda^\mu(p',p)$ into a longitudinal and transverse part

$$\Lambda^\mu(p',p) = \Lambda_L^\mu(p',p) + \Lambda_T^\mu(p',p) , \quad (3.9)$$

where $q_\mu \Lambda_T^\mu(p',p) = 0$. We see that Eq.(2.10) only constrains the longitudinal part. We may consider a form which satisfies Eq. (3.8),

$$\Lambda_L^\mu(p',p) = -\frac{q^\mu}{q^2} (\Sigma(p') - \Sigma(p)) . \quad (3.10)$$

This form is not unique. In reality, the form of $\Lambda^\mu(p',p)$ is significantly more complicated than that given in Eq. (3.10). However, we will make some elementary estimates of the magnitude of vertex corrections in the region of the quasielastic peak based upon Eq. (3.10). A procedure for the calculation of the vertex correction, which will be shown to yield values for $\Lambda^\mu(p',p)$ that satisfy Eq. (3.8), will be given in Section 3.2.

Now we consider the proton vertex, for example, and make use of Eq.(3.10),

$$\Gamma^\mu(p',p) = e \left\{ F_1(q^2) \left[\gamma^\mu - \frac{q^\mu}{q^2} (\Sigma(p') - \Sigma(p)) \right] + i F_2(q^2) \frac{\sigma^{\mu\nu} q_\nu}{2m_N} + \Lambda_T^\mu(p',p) \right\} . \quad (3.11)$$

We remark that $\Lambda_T^\mu(p',p)$ will have terms proportional to both $F_1(q^2)$ and $F_2(q^2)$, in general. Also, we note that we do not here propose a microscopic analysis of $F_1(q^2)$

and $F_2(q^2)$, which would require a QCD-based calculation. Therefore, we do not consider density-dependent modifications of these form factors in this work.

The last two terms of Eq. (3.11) are not constrained by gauge invariance of the theory. Now consider the matrix element

$$q^\mu \bar{f}(\vec{p}', s') \Gamma_\mu(p', p) f(\vec{p}, s) = e F_1(q^2) \bar{f}(\vec{p}', s') [\not{p}' - \not{p} - \Sigma(p') + \Sigma(p)] f(\vec{p}, s) , \quad (3.12)$$

$$= 0 , \quad (3.13)$$

where we have used the Dirac equation satisfied by the $f(\vec{p}, s)$. [We remark that there is an off-mass-shell version of this result where the $f(\vec{p}, s)$ are replaced by the $f(p^0, \vec{p}, s)$ in Eq. (3.12).]

In the next section we provide a diagrammatic analysis for the calculation of $\Sigma(p)$ and $\Lambda^\mu(p', p)$. That analysis provides some insight into the physical processes which appear in the vertex correction and provides a method for a calculation of both the longitudinal and transverse parts of the vertex correction. In order to provide a relatively elementary discussion, we will make use of the Walecka model³.

3.2 Diagrammatic Analysis of Vertex Corrections in Perturbation Theory

In the case of $\sigma+\omega$ model of Walecka³, one can show, in an explicit fashion, that the identity of Eq. (3.7) is satisfied for a specific calculation of the self-energy to be described below. In the more general case, the proof is based upon the fact that the part of the Lagrangian which contains the nucleon field,

$$L(x) = \bar{\psi}_N(x) \left[i\partial_\mu - qA_\mu(x) \right] \gamma^\mu \psi_N(x) - \bar{\psi}_N(x) \left[g_\sigma \sigma(x) + g_\omega \omega_\mu(x) \gamma^\mu \right] \psi_N(x) \quad (3.14)$$

is invariant under phase transformations of the nucleon field, $\psi_N(x)$, leading to the conservation of the electromagnetic current. However, our goal in this section is to show that the Ward-Takahashi identity holds true, term by term, in a perturbative expansion which makes use of the ladder approximation.

It is easy to see that the Ward-Takahashi identity is true to first order in g_σ^2 (or g_ω^2), since $\Sigma^{(1)}(p) = \Sigma^{(1)}(p)$ and , therefore, $\Lambda_\mu^{(1)}(p,p')$ vanishes identically.

[See Fig. 3.1.]

In Fig. 3.2 we show the second order contributions to $\Sigma(p)$ and $\Lambda_\mu(p,p')$,

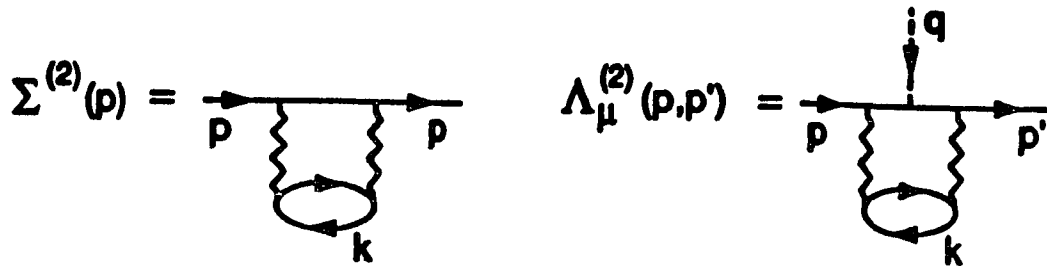


Fig. 3.2

The left-hand part of the figure depicts a second-order contribution to the self-energy. Here k denotes a hole (occupied) state. $\Sigma^{(2)}(p)$ is complex if p refers to a particle above the Fermi sea. The right-hand figure shows the correction to the vertex corresponding to the self-energy $\Sigma^{(2)}(p)$.

$$\Sigma^{(2)}(p) = g_{\sigma}^4 \int \frac{d^4k}{(2\pi)^4} \frac{d^4l}{(2\pi)^4} D(l)G(p-l)D(-l) \text{Tr}[G(k)G(k+l)] \quad (3.15)$$

and

$$\Lambda_{\mu}^{(2)}(p,p') = g_{\sigma}^4 \int \frac{d^4k}{(2\pi)^4} \frac{d^4l}{(2\pi)^4} D(l)G(p-l)\gamma_{\mu}G(p'-l)D(-l) \text{Tr}[G(k)G(k+l)] \quad (3.16)$$

for the case of scalar exchange. Here $D(p)$ is the meson propagator and $G(p)$ is the nucleon propagator in the presence of nuclear matter. For example

$$G(p) = \frac{1}{\not{p} - m + i\eta} + 2\pi i(\not{p} + m)\delta(p^2 - m^2)\Theta(p_F - |\vec{p}|)\Theta(p^0) , \quad (3.17)$$

which can be also written in the intuitive form ¹¹

$$G(p) = \frac{m}{E} \sum_s \left\{ u(\vec{p}, s)\bar{u}(\vec{p}, s) \left[\frac{\Theta(|\vec{p}| - p_F)}{p^0 - E + i\eta} + \frac{\Theta(p_F - |\vec{p}|)}{p^0 - E - i\eta} \right] + \frac{w(\vec{p}, s)\bar{w}(\vec{p}, s)}{p^0 + E - i\eta} \right\} . \quad (3.18)$$

Here $w(\vec{p}, s) \equiv v(-\vec{p}, -s)$. In the limit that $p_F \rightarrow 0$, we recover the propagator in the vacuum,

$$G_0(p) = \frac{1}{\not{p} - m + i\eta} . \quad (3.19)$$

Observing that, from Eq. (3.17),

$$(\not{p} - m) G(p) = 1 , \quad (3.20)$$

one can easily derive the important identity

$$G(p-l) \not{l} G(p-l) = G(p-l) - G(p-l) , \quad (3.21)$$

where $q = p' - p$. (This result is also true for the propagator in the vacuum.) Using Eq. (3.21) in Eq. (3.16), we immediately obtain

$$q^\mu \Lambda_\mu^{(2)}(p, p') = - (\Sigma^{(2)}(p') - \Sigma^{(2)}(p)) . \quad (3.22)$$

We now consider the n^{th} -order contributions, $\Sigma^{(n)}(p)$ and $\Lambda^{(n)}(p, p')$. [See Fig. 3.3]

$$\Sigma^{(n)}(p) = \text{Diagram (a)}$$

(a)

$$\Lambda_{\mu}^{(n)m}(p,p') = \text{Diagram (b)}$$

(b)

Fig. 3.3

- (a) Higher-order corrections to $\Sigma(p)$ calculated in a ladder approximation.
- (b) Corrections to the vertex involving n boson exchanges, with m exchanges appearing to the left of the photon insertion.

The self-energy contribution represented by the diagram in Fig. 3.3a is given by

$$\Sigma^{(n)}(p) = -g_{\sigma}^{2n} \int \frac{d^4k}{(2\pi)^4} \frac{d^4l_1}{(2\pi)^4} \dots \frac{d^4l_{n-1}}{(2\pi)^4} D(l_1) \dots D(l_n) G(p-l_1) \dots G(p-l_1-\dots-l_{n-1})$$

$$\times \text{Tr} [G(k)G(k+l_1) \dots G(k+l_1+\dots+l_{n-1})] . \quad (3.33)$$

The vertex correction has n-1 distinct diagrams corresponding to the n-1 possibilities of distributing the n meson lines on the two proton (particle) lines of the vertex. The diagram represented in Fig. 3.3b is given by

$$\Lambda_{\mu}^{(n)m}(p,p') = g_{\sigma}^{2n} \int \frac{d^4k}{(2\pi)^4} \frac{d^4l_1}{(2\pi)^4} \dots \frac{d^4l_{n-1}}{(2\pi)^4} D(l_1) \dots D(l_n)$$

$$\times G(p-l_1) \dots G(p-l_1-\dots-l_m) \gamma_{\mu} G(p'-l_1-\dots-l_m) \dots G(p'-l_1-\dots-l_{n-1})$$

$$\times \text{Tr} [G(k)G(k+l_1) \dots G(k+l_1+\dots+l_{n-1})] . \quad (3.24)$$

Then, with the help of Eq. (3.21), we obtain

$$q^\mu \Lambda_\mu^{(n)}(p, p') = \sum_{m=1}^{n-1} q^\mu \Lambda_\mu^{(n)m}(p, p') \quad (3.25)$$

$$= g_\sigma^{2n} \int \frac{d^4 k}{(2\pi)^4} \frac{d^4 l_1}{(2\pi)^4} \dots \frac{d^4 l_{n-1}}{(2\pi)^4} D(l_1) \dots D(l_n) \Pi \\ \times \text{Tr} [G(k) G(k+l_1) \dots G(k+l_1+\dots+l_{n-1})] , \quad (3.26)$$

where Π is given by the series:

$$\Pi = \sum_{m=1}^{n-1} G(p-l_1) \dots G(p-l_1-\dots-l_{m-1}) [G(p-l_1-\dots-l_m) - G(p'-l_1-\dots-l_m)] \\ \times G(p'-l_1-\dots-l_{m+1}) \dots G(p'-l_1-\dots-l_{n-1}) . \quad (3.27)$$

If we sum these two series, all terms cancel except the first term of the second series and the last term of the first series. That is,

$$\Pi = G(p-l_1) \dots G(p-l_1-\dots-l_{n-1}) - G(p'-l_1-\dots-l_{m+1}) \dots G(p'-l_1-\dots-l_{n-1}) . \quad (3.28)$$

Thus, we obtain

$$q^\mu \Lambda_\mu^{(n)}(p, p') = - (\Sigma^{(n)}(p') - \Sigma^{(n)}(p)) . \quad (3.29)$$

The proof for the case of ω -exchange or, more generally, for processes involving any number of ω and σ exchanges, is identical except for the addition of Dirac matrices, γ^μ ,

at the ω -nucleon vertices. We note that we may introduce charged mesons, such as π^\pm , in the analysis. A gauge invariant Lagrangian including pions will still preserve the Ward identity; however, the proof of the identity is more complex in that case.

The above perturbative results can be summarized in a compact form by making use of a T matrix of the nucleon-nucleon interaction. As usual, we use the ladder approximation and define the T matrix by the diagrams of Fig. 3.4.

$$\begin{aligned}
 \boxed{T} &= \text{---} \text{---} + \text{---} \text{---} \text{---} + \dots \\
 &= \text{---} \text{---} + \text{---} \boxed{T} \text{---}
 \end{aligned}$$

Fig. 3.4

Schematic representation of the nucleon-nucleon T matrix in the ladder approximation

Then $\Sigma^{(n)}(p)$ and $\Lambda^{(n)}(p,p')$ can be expressed in terms of T [see Figs. 3.5a and 3.5b]

$$\Lambda^\mu(p, p') =$$

(a)

$$\Sigma(p) =$$

(b)

Fig. 3.5

- (a) Representation of the self-energy in terms of the nucleon-nucleon T matrix.
- (b) The vertex correction, $\Lambda^\mu(p', p)$, corresponding to the self-energy shown in (a).

It is seen from our analysis that the wavefunction insertions [Fig. 3.5a], expressed in terms of a T matrix, imply the vertex correction represented here by the insertion of two T matrices, in the manner exhibited in Fig. 3.5b.

3.3 An Estimate of Vertex Corrections Needed in the Presence of Final-State Interactions

We note that the self-energy of Fig. 3.2 will become complex if the nucleon is above the Fermi sea, since excitation of two-particle, one-hole states is then possible. Similarly, $\Lambda_{\mu}^{(2)}(p',p)$ will be complex if $s \equiv (p+q)^2$ is large enough. These observations are also true in the more general case. [See Figs. 3.5a and 3.5 b.]

Let us now estimate the correction which appears as the second term on the right-hand side of Eq. (3.11). Consider $\mu = 0$ and note that $-v/q^2 = 1/(2m_N)$ at the quasielastic peak. For the imaginary part of the correction, we need the matrix element of $[1/(2m_N)] \text{Im}\Sigma(p') \approx [1/(2m_N)] [\text{Im}A + \gamma^0 \text{Im}B]$. This represents about a 1 or 2 percent correction to the leading terms. More precisely, we can form the ratio

$$R = \frac{1}{2m_N} \frac{\bar{f}(\vec{p}',s) [\text{Im}A(p') + \gamma^0 \text{Im}B(p')] f(\vec{p},s)}{\bar{f}(\vec{p}',s)f(\vec{p},s)} \quad (3.30)$$

and use the fact that the $f(\vec{p},s)$ are proportional to free spinors with a shifted mass, in a

first approximation. Then

$$R = \frac{1}{2m_N} [\text{Im}A(p') + \text{Im}B(p')] \quad (3.31)$$

for small values of $|\vec{p}|/(2m_N)$. Note that as we move away from the quasielastic peak to large values of v , v/Q^2 can increase by factors of 2 or 3, yielding somewhat larger corrections than those suggested above. If we consider kinematic regions far from the quasielastic peak, the factor q^4/q^2 can become quite large and estimates based upon the use of Eq. (3.10) may be unreliable.

Chapter 4

One-Body and Many-Body Aspects of the (e,e'p) Reaction: Role of the Ward-Takahashi Identity

4.1 Ward-Takahashi Identity and a Density Expansion for the Vertex Corrections in a Nuclear Medium

Let Σ denote the self-energy of a nucleon in relativistic nuclear matter ¹¹. It is not difficult to show that, if $\gamma^0 \Sigma$ is hermitian, we can introduce a model of the (e,e'p) reaction that is current-conserving. For some purposes, it is useful to define the self-energy for a nucleon in nuclear matter that is in uniform motion. The motion of the medium may be described by the four-vector η_μ . [For example, in the rest frame $\eta_\mu^{\text{RF}} = (1,0,0,0)$ and, in that frame, we can write $\Sigma(p, \eta^{\text{RF}}) = A + \gamma^0 B + \vec{\gamma} \cdot \vec{p} (C/m_N)$, as in our earlier work ¹¹.] Further, we may introduce the spinors $f(p, s, \eta)$ that are solutions of the equation

$$\left[\vec{\gamma} \cdot \vec{p} + m_N + \Sigma(p, \eta) \right] f(p, s, \eta) = \gamma^0 \epsilon(p, \eta) f(p, s, \eta) . \quad (4.1)$$

In this case we write the Ward-Takahashi identity as

$$q^\mu \Lambda_\mu(p, p'; \eta) = - \left[\Sigma(p', \eta) - \Sigma(p, \eta) \right] , \quad (4.2)$$

where Λ_μ denotes the vertex correction. Using Eqs. (4.1) and (4.2), we see that, if $\gamma^0 \Sigma(p, \eta)$ is hermitian, we can show that the current is conserved. That is,

$$q^\mu (\bar{p}', s' | J_\mu(0) | \vec{p}, s) = q^\mu \bar{f}(\vec{p}', s', \eta) \Gamma_\mu(p, p'; \eta) f(\vec{p}, s, \eta) , \quad (4.3)$$

$$= 0 , \quad (4.4)$$

where $\Gamma^\mu(p, p'; \eta)$ denotes the complete vertex operator which, in general, depends on the four-vector η_μ ,

$$\Gamma^\mu(p, p'; \eta) = e \left[\gamma^\mu + \Lambda^\mu(p, p'; \eta) \right] . \quad (4.5)$$

We return to our discussion of the $(e, e'p)$ reaction and note that the optical potential used for the nucleon in the final state is complex (or the corresponding quantity, $\gamma^0 \Sigma$, is nonhermitian), since we wish to describe absorption into channels other than the quasielastic channel. That feature leads to current nonconservation, if we limit ourselves to a one-body model in the calculation of the cross section for the excitation of the quasielastic channel. However, even in the absence of current conservation, the Ward-Takahashi identity can still be seen to be valid in certain cases. The reason for creating a model that satisfies that identity, even in the case that the single-channel analysis is not charge-conserving, is that the identity constrains the

theory to describe important aspects of the dynamics properly. That will become clear as we proceed with our discussion; however, we may make some qualitative comments at this point.

We note that the same interaction which mediates the collisions of the outgoing proton with other nucleons of the medium is responsible for the admixture of two-particle, two-hole (2p-2h) states into the ground state. That feature leads to a reduced occupation probability for the occupied states and, therefore, a wave function renormalization constant for these states appears in the formalism. For consistency, we should allow the virtual photon to create a particle-hole configuration and also couple the photon to the configurations of 2p-2h character. Both these processes may lead to the same final state. [See Fig. 4.1.] It will be seen that some of these additional terms that arise, when we consider the 2p-2h components of the ground state, appear as vertex corrections in this formalism. Indeed, the Ward-Takahashi identity allows one to identify the specific vertex corrections that should be taken into account, if one adopts a specific model for the self-energy.

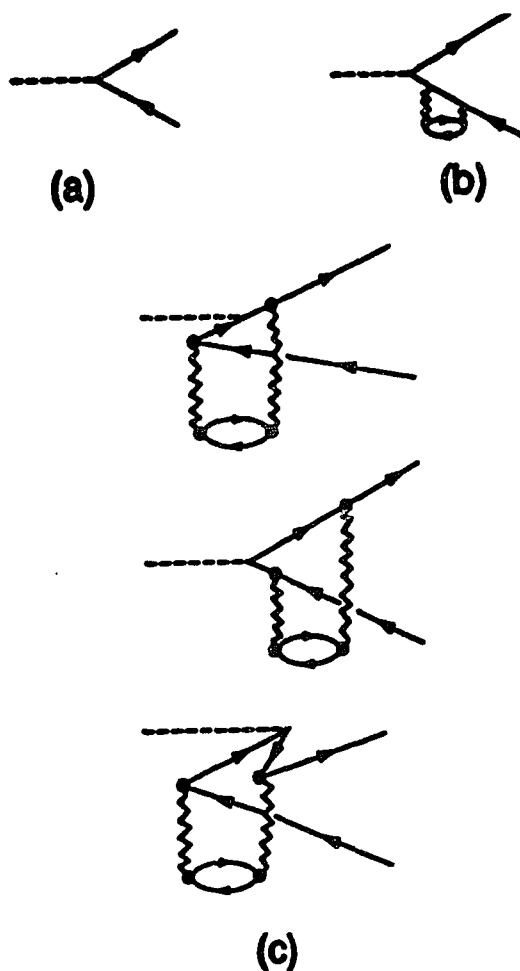
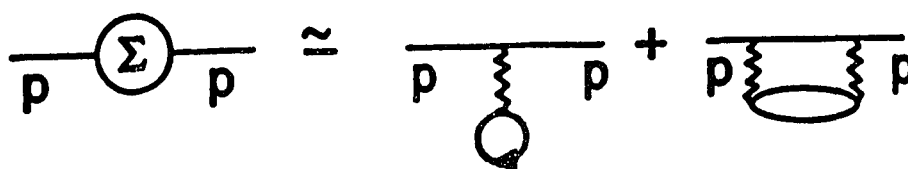


Fig. 4.1

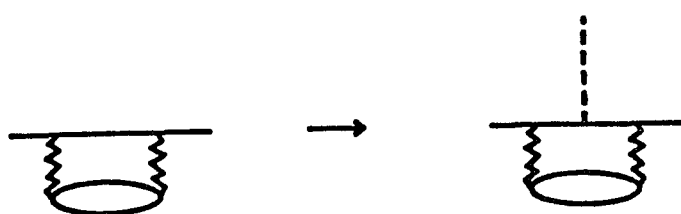
- a) Goldstone diagram for the excitation of a particle-hole state by an incident photon (dashed line).
- b) Diagram denoting a wave function renormalization insertion on the hole line. The wavy line denotes a meson propagator. (We neglect retardation in the meson propagator.)
- c) Goldstone diagrams for some of the vertex corrections, containing two meson lines, that should be considered if final-state interactions are calculated to the same order.

The virtue of our analysis, made for an (interacting) relativistic Fermi gas, lies in the fact that we can identify the diagrams that correspond to the insertion of optical potentials for the outgoing nucleon. [In the Fermi gas model, the quantity which corresponds to the optical potential is $\gamma^0 \Sigma(p)$.]

In order to simplify the analysis, we consider a model of nucleons interacting with scalar mesons. In our earlier work ¹⁵ we considered the insertions in the external lines of the relevant diagram to be of the form shown in Fig. 4.2(a). In the case the external line represents an occupied state, these insertions will be real; however, if the particle is above the Fermi sea, the second diagram on the right-hand side of Fig. 4.2(a) may be complex, corresponding to the excitation of an open channel - an intermediate state of two-particle, two-hole character. If we consider an occupied state, the second diagram in Fig. 4.2(a) serves to represent the dynamics which lead to a reduced occupation probability of that state, and gives rise to a wave function renormalization constant, or spectroscopic factor. Also, as discussed in our earlier work ¹⁵ on this topic, we see that the Ward-Takahashi identity is satisfied, if the vertex correction is made as is shown in Fig. 4.2(b). For the processes shown in that figure, we have the relation between the vertex correction and the self-energy that is given in Eq. (4.2). That is to say, there are certain diagrams (self-energy insertions and vertex corrections) which are related by the Ward-Takahashi identity.



(a)



(b)



(c)

Fig. 4.2

- a) Many-body Feynman diagrams for the calculation of the self-energy Σ . The first diagram is independent of momentum. The second diagram, which may represent a final-state interaction, is discussed in this work.
- b) The vertex correction, corresponding to the self-energy insertion on the left, is shown. The dashed line denotes a photon.
- c) A meson vacuum polarization diagram. The density-dependent part of this diagram is considered in this work. [See Sec. 4.2.]

In this chapter we are interested in developing procedures for the calculation of the diagrams shown in Fig. 4.2(b). As will be demonstrated, it is possible to simplify the calculation by making a systematic expansion in terms of the density of the nuclear medium. It is also useful to limit our discussion to the kinematic region where we may neglect the dependence of the meson propagator on the zeroth component of the momentum, k^0 . With the neglect of retardation in the meson propagator, we may relate the many-body Feynman diagrams of Fig. 4.2 to the Goldstone diagrams of Fig. 4.1 by completing the integrals over the zeroth components of the various internal momentum. A further simplification is to assume that the nucleon energies are nonrelativistic, so that the density-dependent part of the meson self-energy [see Fig. 4.2(c)] may be approximated by the nonrelativistic Lindhard function. (A detailed calculation of that function is presented in Ref. 16, for example.) We use the many-body, field-theoretic formalism presented in Ref. 16, as extended to describe a relativistic system in Ref. 11.

It is useful to write the nucleon propagator, in the presence of infinite nuclear matter, in the form

$$G(p) = \frac{i}{\not{p} - m_N + i\epsilon} - 2\pi(\not{p} + m)\delta(p^2 - m_N^2)\Theta(p^0)\Theta(p_F - |\vec{p}|) \quad (4.6)$$

$$\equiv G_0(p) + G_n(p) \quad (4.7)$$

Here $G_0(p)$ is the free nucleon propagator and $G_n(p)$ is the part of $G(p)$ that depends on the density of nuclear matter. We use the four-vector η_μ to rewrite Eq. (4.6) in a covariant form (see Fig. 4.3),

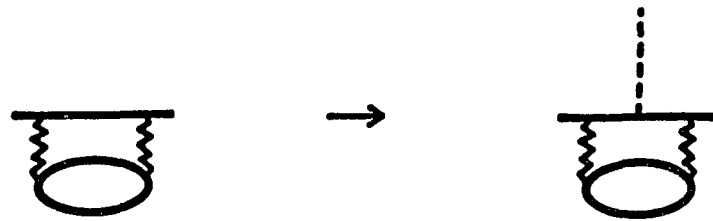
$$G(p) = G_0(p) - 2\pi(\not{p} + m)\delta(p^2 - m^2)\Theta(p \cdot \eta)\Theta(p^2 + p^2 - (p \cdot \eta)^2) \quad (4.8)$$

(For simplicity, we use the notation $G(p)$, rather than $G(p, \eta)$. Note that the introduction of the vector η_μ facilitates the evaluation of various integrals, as described in Section 4.2.) As indicated in Fig. 4.3, the second term in Eq. (4.8) is represented by a filled circle placed on a nucleon line. Therefore, by counting the number of such elements in a diagram, we may make a systematic expansion in the density of the medium. [See Fig. 4.4.]

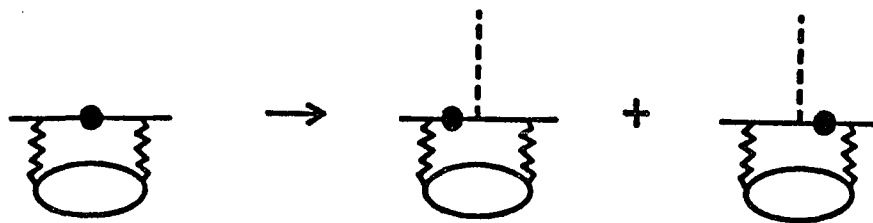


Fig. 4.3

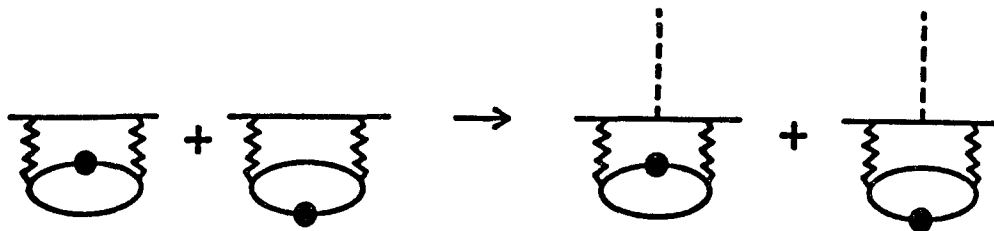
Representation of the Green's function of Eq. (4.8), $G(p)$, in terms of the free Green's function, $G_0(p)$, and a density-dependent correction, $G_n(p, \eta)$, denoted by a filled circle. [See Eq. (4.8).]



(a)



(b)



(c)

Fig. 4.4

a) Self-energy insertion and the corresponding vertex correction.
 b) and c) Self-energy insertions and the corresponding vertex corrections calculated to lowest order in the density of the medium. [See Fig.4.3 and Eq. (4.8).]

In this chapter, we consider nucleons interacting with sigma mesons. Since the σ -meson is neutral, we need not consider meson-exchange currents in this model. Consider the diagrams of Fig. 4.4(c). These diagrams involve the density-dependent part of the σ -meson polarization, Π . It is useful to define the scalar quantity

$$\Pi(k,\eta) = ig_{\sigma}^2 \int \frac{d^4l}{(2\pi)^4} \text{Tr} [G(k+l)G(l) - G_0(k+l)G_0(l)] , \quad (4.9)$$

$$\approx ig_{\sigma}^2 \int \frac{d^4l}{(2\pi)^4} \text{Tr} [G_0(k+l)G_n(l) - G_n(k+l)G_0(l)] , \quad (4.10)$$

which vanishes in the absence of nuclear matter.

We now consider the sum of the density-dependent parts of the vertex correction and the self-energy shown in Fig. 4.2(b) and 4.2(c). We have

$$\Lambda_{\mu}(p,p';\eta) = ig_{\sigma}^2 \int \frac{d^4k}{(2\pi)^4} D^2(k)\Pi(k,\eta)G(p'-k)\gamma_{\mu}G(p-k) \quad (4.11)$$

and

$$\Sigma(p,\eta) = -g_{\sigma}^2 \int \frac{d^4k}{(2\pi)^4} D^2(k)\Pi(k,\eta)G(p-k) . \quad (4.12)$$

Here $D(k)$ is the σ -meson propagator.

Using the relation

$$G(p'-k) \not{\partial} G(p-k) = i [G(p-k) - G(p'-k)] \quad (4.13)$$

we see that $\Lambda_\mu(p,p';\eta)$ and $\Sigma(p,\eta)$ of Eq. (4.11) and (4.12) satisfy the Ward-Takahashi identity, Eq. (4.2). We now concentrate on the diagrams of Fig. 4.4(c) and write

$$\Lambda_\mu(p,p';\eta) = ig_\sigma^2 \int \frac{d^4k}{(2\pi)^4} D^2(k)\Pi(k,\eta)G_0(p'-k)\gamma_\mu G_0(p-k) \quad (4.14)$$

and

$$\Sigma(p,\eta) = -g_\sigma^2 \int \frac{d^4k}{(2\pi)^4} D^2(k)\Pi(k,\eta)G_0(p-k) , \quad (4.15)$$

where $\Pi(k,\eta)$ is given by Eq. (4.9) and may be approximated as in Eq. (4.10). Note that the quantities given in Eqs. (4.14) and (4.15) separately satisfy the Ward-Takahashi identity, since Eq. (4.13) is also true for the free Green's functions, $G_0(p'-k)$ and $G_0(p-k)$. We, therefore, note the advantage obtained in using many-body Feynman diagrams rather than Goldstone diagrams, such as those of Fig. 4.1. (Since the individual Goldstone diagrams do not satisfy a Ward-Takahashi identity, it would be quite difficult to organize a calculation, based upon the use of Goldstone diagrams, so as to insure that the identity is satisfied.)

4.2 Evaluation of the Vertex Corrections in a Nuclear Medium

We now proceed to calculate the form of Λ_μ , the correction to the photon-nucleon vertex. We first replace γ_μ in Eq. (4.14) by

$$\Gamma_\mu = \gamma_\mu F_1(q^2) + i \frac{\sigma_{\mu\nu}}{2m_N} q^\nu F_2(q^2) \quad . \quad (4.16)$$

If we keep in mind that we will eventually need matrix elements of Λ_μ taken between free spinors, $\bar{u}(p')$ and $u(p)$, the vertex correction takes the form,

$$\Lambda_\mu(p,p';\eta) = -ig_\sigma^2 \int \frac{d^4k}{(2\pi)^4} D^2(k) \Pi(k,\eta) \frac{2m_N - \not{k}}{k^2 - 2k \cdot p} \left[\gamma_\mu F_1 + i \frac{\sigma_{\mu\nu}}{2m_N} q^\nu F_2 \right] \frac{2m_N - \not{k}}{k^2 - 2k \cdot p} \quad . \quad (4.17)$$

Here we have used the Dirac equation satisfied by the spinors, $\bar{u}(p')$ and $u(p)$ and have also taken the incoming and outgoing nucleons to be on shell: $p^2 = p'^2 = m^2$. We can simplify the structure of the integrand in Eq. (4.17) by noting that,

$$\left[1 - \frac{\not{k}}{2m_N} \right] \gamma_\mu \left[1 - \frac{\not{k}}{2m_N} \right] = -\frac{k_\mu}{m_N} + \gamma_\mu \left[1 - \frac{k^2}{4m_N^2} \right] + \frac{\gamma^\nu k_\nu k_\mu}{2m_N^2} \quad (4.18)$$

and

$$\left[1 - \frac{\not{k}}{2m_N}\right] \sigma_{\mu\nu} \left[1 - \frac{\not{k}}{2m_N}\right] = \sigma_{\mu\nu} \left[1 + \frac{k^2}{4m_N^2}\right] + \varepsilon_{\tau\mu\nu\rho} \gamma^\tau \gamma_5 \frac{k^\rho}{m_N} + (\sigma_{\rho\mu} k_\nu - \sigma_{\rho\nu} k_\mu) \frac{k^\rho}{2m_N^2} . \quad (4.19)$$

If we make use of these relations, the integrand of Eq. (4.17) consists of three types of terms: scalars, vectors (proportional to k_ρ), and tensors (proportional to $k_\rho k_\sigma$).

To simplify the integration we define a set of orthogonal four-vectors

$$\pi = p + p' , \quad (4.20)$$

$$q = p - p' , \quad (4.21)$$

and

$$\rho = \eta - q \left(\frac{\eta \cdot q}{q^2} \right) - \pi \left(\frac{\eta \cdot \pi}{\pi^2} \right) . \quad (4.22)$$

Since the integrals are manifestly Lorentz covariant, they can be expressed completely in terms of π^μ , q^μ , and ρ^μ . For scalar integrals, the result is of the form

$$I_s \equiv \int d^4k F(p \cdot k, p' \cdot k, k^2, k \cdot \eta) = \Phi(q^2, q \cdot \eta, \pi \cdot \eta) . \quad (4.23)$$

[The dependence on $q \cdot \eta$ and $\pi \cdot \eta$ is necessary due to the definition of Eq. (4.22).]

The evaluation of the vector integrals can be reduced to the evaluation of scalar integrals,

since

$$I_V^\mu \equiv \int d^4k F(p \cdot k, p' \cdot k, k^2, k \cdot \eta) k^\mu, \quad (4.24)$$

$$= \pi^\mu \Phi_\pi(q^2, q \cdot \eta, \pi \cdot \eta) + q^\mu \Phi_q(q^2, q \cdot \eta, \pi \cdot \eta) + \rho^\mu \Phi_\rho(q^2, q \cdot \eta, \pi \cdot \eta), \quad (4.25)$$

$$= \int d^4k F(p \cdot k, p' \cdot k, k^2, k \cdot \eta) \left[\frac{k \cdot \pi}{\pi^2} \pi^\mu + \frac{k \cdot q}{q^2} q^\mu + \frac{k \cdot \rho}{\rho^2} \rho^\mu \right]. \quad (4.26)$$

Equation (4.26) follows from the identification $\Phi_\pi = (I_V^\mu \cdot \pi_\mu / \pi^2)$, etc. To reduce the tensor integrals

$$I_i^{\mu\nu} \equiv \int d^4k F(p \cdot k, p' \cdot k, k^2, k \cdot \eta) k^\mu k^\nu \quad (4.27)$$

to scalar integrals, in a similar fashion, it is convenient to define a complete set of symmetric tensors, $T_i^{\mu\nu}$, in terms of π_μ , q_μ , and ρ_μ . These tensors are constructed

so that

$$\text{Tr} (T_i T_j) = \delta_{ij} . \quad (4.28)$$

Such a set is, for example:

$$T_1^{\mu\nu} = \frac{q^\mu q^\nu}{q^2} , \quad (4.29)$$

$$T_2^{\mu\nu} = \frac{1}{\sqrt{3}} \left[g^{\mu\nu} - T_1^{\mu\nu} \right] , \quad (4.30)$$

$$T_3^{\mu\nu} = \frac{1}{\sqrt{2}} \left[\sqrt{3} \frac{\pi^\mu \pi^\nu}{\pi^2} - T_2^{\mu\nu} \right] , \quad (4.31)$$

$$T_4^{\mu\nu} = \frac{\sqrt{2}}{\sqrt{3}} \left[\sqrt{3} \frac{\rho^\mu \rho^\nu}{\rho^2} - T_2^{\mu\nu} + T_3^{\mu\nu} \right] , \quad (4.32)$$

$$T_5^{\mu\nu} = \frac{1}{\sqrt{2}} \left[\frac{\rho^\mu \pi^\nu + \rho^\nu \pi^\mu}{(\rho^2 \pi^2)^{1/2}} \right] , \quad (4.33)$$

$$T_6^{\mu\nu} = \frac{1}{\sqrt{2}} \left[\frac{q^\mu \pi^\nu + q^\nu \pi^\mu}{(q^2 \pi^2)^{1/2}} \right] , \quad (4.34)$$

$$T_7^{\mu\nu} = \frac{1}{\sqrt{2}} \left[\frac{\rho^\mu q^\nu + \rho^\nu q^\mu}{(\rho^2 q^2)^{1/2}} \right] . \quad (4.35)$$

Then the tensor integral, $I_T^{\mu\nu}$ of Eq. (4.27), can be expressed in terms of the tensors of Eqs. (4.29) - (4.35),

$$I_T^{\mu\nu} = \sum_{i=1}^7 T_i^{\mu\nu} \Phi_i(q^2, q \cdot \eta, \pi \cdot \eta) , \quad (4.36)$$

where the coefficients, Φ_i , are given by

$$\Phi_i(q^2, q \cdot \eta, \pi \cdot \eta) = T_{\mu\nu, i} I_T^{\mu\nu} . \quad (4.37)$$

Thus, the tensor integrals can be reduced to a sum of scalar integrals of the form:

$$I_T^{\mu\nu} = \sum_{i=1}^7 T_i^{\mu\nu} \int d^4k F(p \cdot k, p' \cdot k, k^2, k \cdot \eta) (k_\rho T_i^{\rho\sigma} k_\sigma) . \quad (4.38)$$

The tensor structure in the above expression can be somewhat simplified, if we use the relation

$$\begin{aligned}
\sum_{i=1}^7 T_i^{\rho\lambda} (k_\nu T_i^{\nu\eta} k_\eta) = & g^{\rho\lambda} \left[k^2 - \frac{(q \cdot k)^2}{q^2} - \frac{(\pi \cdot k)^2}{\pi^2} - \frac{(\rho \cdot k)^2}{\rho^2} \right] \\
& - \frac{q^\rho q^\lambda}{q^2} \left[k^2 - 2 \frac{(q \cdot k)^2}{q^2} - \frac{(\pi \cdot k)^2}{\pi^2} - \frac{(\rho \cdot k)^2}{\rho^2} \right] \\
& - \frac{\pi^\rho \pi^\lambda}{\pi^2} \left[k^2 - \frac{(q \cdot k)^2}{q^2} - 2 \frac{(\pi \cdot k)^2}{\pi^2} - \frac{(\rho \cdot k)^2}{\rho^2} \right] \\
& - \frac{\rho^\rho \rho^\lambda}{\rho^2} \left[k^2 - \frac{(q \cdot k)^2}{q^2} - \frac{(\pi \cdot k)^2}{\pi^2} - 2 \frac{(\rho \cdot k)^2}{\rho^2} \right] \\
& + (\rho^\rho \pi^\lambda + \rho^\lambda \pi^\rho) \frac{(\rho \cdot k) (\pi \cdot k)}{\rho^2 \pi^2} \\
& + (\rho^\rho q^\lambda + \rho^\lambda q^\rho) \frac{(\rho \cdot k) (q \cdot k)}{\rho^2 q^2} \\
& + (\pi^\rho q^\lambda + \pi^\lambda q^\rho) \frac{(\pi \cdot k) (q \cdot k)}{\pi^2 q^2} .
\end{aligned}
\tag{4.39}$$

Once all integrals have been reduced to the evaluation of scalar quantities, we proceed to perform the integration over k^0 . The integrand includes the σ -meson polarization insertion $\Pi(k, \eta)$ given by the Lindhard function ¹⁶. This has a real and an imaginary part. The real part is:

$$\begin{aligned} \text{Re } \Pi(k) = \frac{m_N k_F}{2\pi^2} & \left\{ -1 + \frac{1}{2x} \left[1 - \left(\frac{y}{x} - \frac{x}{2} \right)^2 \right] \ln \left| \frac{1 + \left(\frac{y}{x} - \frac{x}{2} \right)}{1 - \left(\frac{y}{x} - \frac{x}{2} \right)} \right| \right. \\ & \left. - \frac{1}{2x} \left[1 - \left(\frac{y}{x} + \frac{x}{2} \right)^2 \right] \ln \left| \frac{1 + \left(\frac{y}{x} + \frac{x}{2} \right)}{1 - \left(\frac{y}{x} + \frac{x}{2} \right)} \right| \right\} \end{aligned} \quad (4.40)$$

where $x = |\vec{k}|/k_F$ and $y = mk_0/k_F^2$. By appropriate transformations, the integrals that appear when evaluating the real part of $\Pi(k)$ can be reduced to integrals over an analytic function using the formula

$$\int_{-\infty}^{\infty} dx f(x) \ln|x| = -\frac{1}{2} \oint dz \{ [f(z) + f(-z)] \ln z - i\pi f(z) \} \quad (4.41)$$

This integral can be then evaluated through ordinary contour integration, selecting a contour that does not cross the branch cut due to the presence of $\ln z$ in Eq. (4.41). The imaginary part of $\Pi(k)$,

$$\begin{aligned} \text{Im } \Pi(k) = -\frac{m_N k_F}{4\pi x} & \left\{ 2y\Theta(y)\Theta(2-x)\Theta\left(x - \frac{x^2}{2} - y\right) + \left[1 - \left(\frac{y}{x} - \frac{x}{2} \right)^2 \right] \right. \\ & \left. \times \Theta\left(x + \frac{x^2}{2} - y\right) \left[\Theta(x-2)\Theta\left(y + x - \frac{x^2}{2}\right) + \Theta(2-x)\Theta\left(y - x + \frac{x^2}{2}\right) \right] \right\} , \end{aligned} \quad (4.42)$$

is not an analytic function of k_0 and the method of taking the principal part is employed to separate the singularities that arise in the propagators. The resulting integral and the remaining integration over \vec{k} is to be performed numerically. The principal part of an integral is obtained through the identity

$$P \int_{-\infty}^{\infty} \frac{f(x)}{x-a} dx = \int_{-\infty}^{\infty} \frac{f(x) - f(a)}{x-a} dx . \quad (4.43)$$

4.3 Many-Body Aspects of the Dynamics

Apart from the diagrams of Fig. 4.1(c) there exists the possibility that the virtual photon couples to the fermion loop [see Fig. 4.5(a), (b)]. Thus, there are additional vertex corrections unaccounted for in our preceding analysis. In this section, we comment on these additional corrections.

It can be easily demonstrated that these corrections vanish in the vacuum: The Feynman diagrams depicted in Figs. 4.6(a) and 4.6(b) give,

$$T_{\mu}(p,p') = -ie g_{\sigma}^2 \int \frac{d^4 k}{(2\pi)^4} \left\{ \text{Tr} \left[G_0(k+p) \gamma_{\mu} G_0(k+p') G_0(k) \right] \right. \\ \left. + \text{Tr} \left[G_0(k-p) \gamma_{\mu} G_0(k-p) G_0(k) \right] \right\} \quad (4.44)$$

By rearranging the order of the propagators in the second term, we obtain

$$T_{\mu}(p,p') = -ie g_{\sigma}^2 \int \frac{d^4k}{(2\pi)^4} \text{Tr} \left[G_0(k+p) \gamma_{\mu} G_0(k+p') G_0(k) \right. \\ \left. + G_0(k-p) \gamma_{\mu} G_0(k-p') G_0(k) \right] . \quad (4.45)$$

The second term in Eq. (4.45) may be obtained from the first, if we make the substitution $p \rightarrow -p$ and $p' \rightarrow -p'$. After performing the integration in Eq. (4.45), we see that the first term of Eq. (4.45) is constrained to be of the form

$$T_{\mu}^{(1)}(p,p') = (p_{\mu} + p'_{\mu}) f(p \cdot p', p^2, p'^2) , \quad (4.46)$$

since the result should be symmetrical under the interchange of p and p' . Consequently, the sum of the two terms in Eq. (4.45) vanishes,

$$T_{\mu}(p,p') = T_{\mu}^{(1)}(p,p') + T_{\mu}^{(1)}(-p,-p') = 0 . \quad (4.47)$$

However, this proof does not hold in the case that the nucleon propagation takes place in nuclear matter, since the four-vector describing the motion of the nuclear medium, η_{μ} , appears as an extra variable in T_{μ} . The generalization of Eq. (4.46) in the presence of nuclear matter is

$$\begin{aligned}
T_{\mu}^{(1)}(p,p',\eta) &= (p_{\mu} + p'_{\mu}) f(p \cdot p', p^2, p'^2, p \cdot \eta, p' \cdot \eta) \\
&+ \eta_{\mu} g(p \cdot p', p^2, p'^2, p \cdot \eta, p' \cdot \eta)
\end{aligned} \tag{4.48}$$

where the functions f and g are symmetric under the interchange of p and p' . In this case the sum of the two diagrams of Fig. 4.6 is

$$\begin{aligned}
T_{\mu}(p,p',\eta) &= (p_{\mu} + p'_{\mu}) \left[f(p \cdot p', p^2, p'^2, p \cdot \eta, p' \cdot \eta) - f(p \cdot p', p^2, p'^2, -p \cdot \eta, -p' \cdot \eta) \right] \\
&+ \eta_{\mu} \left[g(p \cdot p', p^2, p'^2, p \cdot \eta, p' \cdot \eta) - g(p \cdot p', p^2, p'^2, -p \cdot \eta, -p' \cdot \eta) \right]
\end{aligned} \tag{4.49}$$

which is nonzero. One can obtain T_{μ} in the rest frame of the nuclear medium by setting $\eta_{\mu} = (1,0,0,0)$. However, even though $T_{\mu}(p,p',\eta)$ is nonzero in nuclear matter, one can easily check that the Ward-Takahashi Identity, Eq.(4.2), is still satisfied.

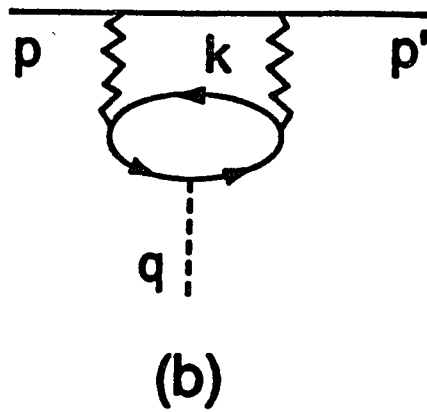
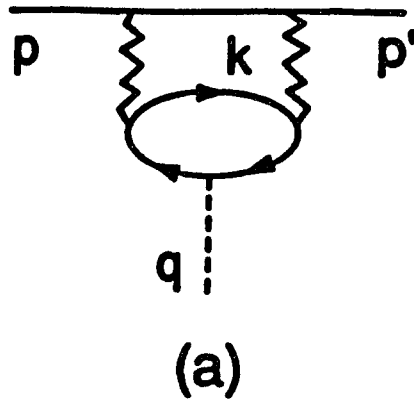
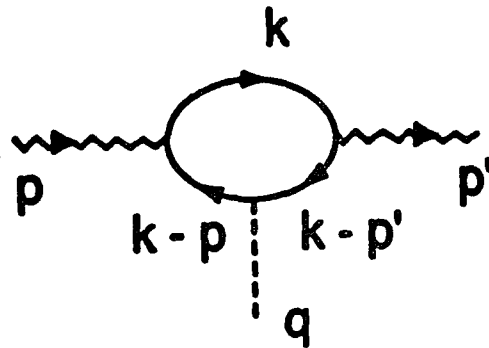
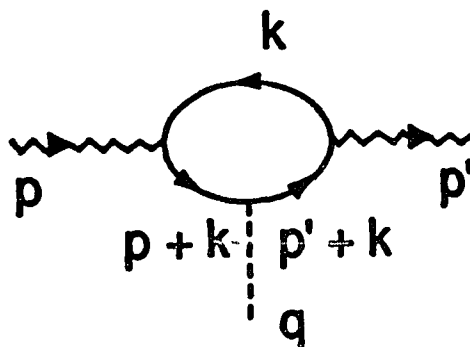


Fig. 4.5

Vertex corrections in which the photon of momentum q couples to a polarization insertion in the meson line. Here the arrows denote the direction of the momentum flow. As discussed in the text, the sum of the two diagrams vanishes in the vacuum.



(a)



(b)

Fig. 4.6

Portions of the diagrams of Fig. 4. 5 are here drawn as photon-meson vertex corrections. The sum of these diagrams may be shown to vanish if $\eta_\mu = \eta_\mu^{RF} = (1,0,0,0)$, $q^0 = 0$ and $p^2 = p'^2 = m^2$. [See the Sec. 4.3.]

Consider the vertex corrections depicted in Figs.4.5(a) and 4.5(b),

$$\Lambda_{\mu}(p,p') = ie g_{\sigma}^4 \int \frac{d^4l}{(2\pi)^4} \frac{d^4k}{(2\pi)^4} D(l)G(p-l)D(l')$$

$$\times \text{Tr} \left[G(k+l)\gamma_{\mu}G(k+l')G(k) + G(k-l)\gamma_{\mu}G(k-l')G(k) \right]$$
(4.50)

where $l' = l+q$. Multiplying by q^{μ} and using Eq.(4.13), we obtain

$$q^{\mu}\Lambda_{\mu}(p,p') = -e g_{\sigma}^4 \int \frac{d^4l}{(2\pi)^4} \frac{d^4k}{(2\pi)^4} D(l)G(p-l)D(l')$$

$$\times \text{Tr} \left\{ \left[G(k+l') - G(k+l) \right] G(k) + \left[G(k-l) - G(k-l') \right] G(k) \right\} .$$
(4.51)

By defining variables $k-l = \tilde{k}$ and $k-l' = \tilde{k}'$ in the third and fourth term of the trace respectively, we see that the trace vanishes. Thus this vertex correction does not contribute to the Ward-Takahashi identity which relates the nucleon self energy and vertex correction depicted in Fig 4.4(a). This is to say, we have $q^{\mu}\Lambda_{\mu}(p',p) = 0$ for those vertex corrections for which there is no corresponding self-energy term. Finally, we note that there will be some degree of suppression of the contribution of the diagrams of Figs. 4.5(a) and 4.5(b) when q^2 is large, if we include meson-nucleon form factors in the formalism.

Chapter 5

Discussion and Conclusions

Our goal in this work has been, in part, to understand the dynamics underlying the calculations reported by Chinn, Picklesimer and Van Orden by studying the role of final-state interactions in corresponding calculations made for nuclear matter. The essential features of the results found in the case of finite nuclei ⁷ are reproduced in our study. However, nuclear matter studies have the virtue that the calculations can be improved in the direction of creating a charge-conserving analysis. Methods for satisfying the Ward-Takahashi identity in calculations of the type considered here, where particle knockout dominates the final-state interaction, have been given. In a future work we hope to study whether the results reported here will be modified in a calculation which includes the vertex corrections that are required in an analysis which preserves the Ward-Takahashi identity. Further, as noted in Ref. 7, a fully satisfactory theory of $(e,e'p)$ reactions has not been developed. We hope that this analysis, supplemented by calculations of vertex corrections ¹⁵, will assist in the formulation of a more satisfactory theory than exists presently.

We have made some elementary estimates of the corrections required for electromagnetic vertices due to the presence of a nuclear medium. While detailed calculations of such vertex corrections may be made in the case of nuclear matter, these corrections appear to be small in the region governed by the quasielastic response. (Clearly, it would be desirable to carry out a similar analysis for a finite system;

however, in that case the ease of analysis found in the case of nuclear matter is not present.)

One useful feature of our analysis is that it provides a method for the calculation of $\Lambda_\mu(p,p')$, since we have identified the specific vertex corrections required when $\Sigma(p)$ is calculated as in Fig. 3.5 (b). [This diagram may be put into correspondence with the leading contributions to the phenomenological optical potential used to describe final-state interactions in the case of nucleon ejection from finite nuclei¹¹.] One unsatisfactory feature of our discussion is seen in the observation that Eq. (3.10) is not the only form which satisfies Eq. (3.8). Therefore, for a definitive analysis it is necessary to actually calculate the vertex corrections in the manner outlined in Section 3.2. Such calculations are difficult, but are necessary if one is to make a fully consistent calculation of the electromagnetic response functions.

In addition, we note that the role of the Ward-Takahashi identity in the relativistic two-body problem has been discussed in the works of Ref. 13. However, the program considered in those works is quite different from that considered here.

We have studied the vertex corrections which correspond to the self-energy insertion in Fig. 4.4(a). In particular, we have indicated how the vertex corrections shown on the right-hand side of Fig. 4.4(b) may be calculated. From the discussion of Sec. 4.2 it may be seen that a rather complex structure emerges for the vertex correction, $\Lambda_\mu(p,p';\eta)$. The correction terms are of the same order in the density and coupling constant as the self-energy insertion. Although we do not present any

numerical calculations in this work, we may conclude that the conventional methods used in the calculation of the $(e,e'p)$ process should be improved by calculating the vertex corrections which may lead to effects of the same order of magnitude as those originating from the use of optical potentials to describe the interaction of the final-state nucleon with the residual system. At this point, we suggest that these vertex corrections be calculated for nuclear matter, with $\eta_{\mu} = \eta_{\mu}^{\text{RF}}$, since it is unclear as to how to extend the analysis given here to the calculation of the $(e,e'p)$ process for finite nuclei. We believe that such calculations are necessary, if the $(e,e'p)$ reaction is to be useful in obtaining accurate spectroscopic factors¹⁷.

Finally, we note that the effective one-body model discussed here is not charge-conserving. Therefore, it appears necessary to calculate amplitudes other than those defining the effective one-body model. More precisely, one should consider the excitation of two-particle, two-hole states in addition to the excitation of one-particle, one-hole states. That program has not been considered in this work.

Appendix

In this Appendix we present the values used for the real and imaginary parts of $A(\vec{p})$, $B(\vec{p})$ and $C(\vec{p})$. These values are obtained by constructing analytic expressions which (approximately) fit the numerical results given in Ref. 5. The fit is made for $k_F = 1.36 \text{ fm}^{-1}$. If the density considered is less than that of nuclear matter, we use the approximation $A(\rho, \vec{p}) = (\rho/\rho_{NM}) A(\rho_{NM}, \vec{p})$, etc. We chose, for $\rho = \rho_{NM}$,

$$\text{Re } A(\vec{p}) = \left[-340 + 3.05 \times 10^{-4} \vec{p}^2 \right] \text{ MeV}, \quad 0 < |\vec{p}| \leq 3.25 \text{ fm}^{-1}. \quad (\text{A.1})$$

$$\text{Im } A(\vec{p}) = \frac{-54.67 (|\vec{p}| - k_F)^2}{(|\vec{p}| - k_F)^2 - 8.18 \times 10^5} \text{ MeV}, \quad k_F < |\vec{p}| < 2.25 \text{ fm}^{-1}; \quad (\text{A.2})$$

$$= \frac{162.3 (|\vec{p}| - k_F)^2}{(|\vec{p}| - k_F)^2 + 2.02 \times 10^5} \text{ MeV}, \quad 2.25 \text{ fm}^{-1} < |\vec{p}| < 3.25 \text{ fm}^{-1}. \quad (\text{A.3})$$

$$\text{Re } B(\vec{p}) = \left[260 - 2.78 \times 10^{-4} |\vec{p}|^2 \right] \text{ MeV}, \quad 0 \leq |\vec{p}| \leq 3.25 \text{ fm}^{-1}. \quad (\text{A.4})$$

$$\text{Im } B(\vec{p}) = \frac{-141.2 (|\vec{p}| - k_F)^2}{(|\vec{p}| - k_F)^2 + 7.20 \times 10^4} \text{ MeV}, \quad k_F < |\vec{p}| < 2.75 \text{ fm}^{-1}; \quad (\text{A.5})$$

$$\text{Im } B(\vec{p}) = \frac{-203.2 (|\vec{p}| - k_F)^2}{(|\vec{p}| - k_F)^2 + 1.37 \times 10^5} \text{ MeV}, \quad 2.75 \text{ fm}^{-1} \leq |\vec{p}| \leq 3.25 \text{ fm}^{-1} .$$

(A.6)

REFERENCES

1. B. Frois and C. N. Papanicolas, Ann. Rev. Nucl. Part. Sci. **37**, 133 (1987).
2. G. Do Dang and N. Van Gial, Phys. Rev. C30, 731 (1984).
3. J. D. Walecka, Ann. Phys. (NY) 83, 491 (1974);
B. D. Serot, and J. D. Walecka, Adv. Nucl. Phys. Vol.16 (Plenum Press, New York, 1986).
4. L. S. Celenza, et al., Phys. Rev. C31, 232 (1985).
5. S. Fantoni and V. R. Pandharipande, Nucl. Phys. A473, 234 (1987).
6. Y. Horikawa, et al., Phys. Rev. C22, 1680 (1980).
7. C. R. Chinn, A. Picklesimer, and J. W. Van Orden, Phys. Rev. C40, 790 (1989).
This work contains very extensive references to the experimental and theoretical literature.
8. X. Song, J. P. Chen, P. K. Kabir and J. S. McCarthy, Univ. of Virginia Preprint (1990).
C. R. Chinn and A. Picklesimer, Lawrence Livermore National Laboratory, preprint: UCRL-JC-106072 (1990).
9. For a comprehensive discussion of sum rules in both nonrelativistic and relativistic theories, see C. R. Chinn, A. Picklesimer, and J. W. Van Orden, Phys. Rev. C40, 1159 (1989).
10. L. S. Celenza, A. Pantziris, C. M. Shakin, and Hui-wen Wang, Phys. Rev. C43, 1367 (1991).
11. L. S. Celenza, C. M. Shakin, Relativistic Nuclear Physics: Theories of Structure and Scattering, (World Scientific, Singapore, 1986).
12. W. Bentz, A. Arima, H. Hyuga, K. Shimizu, and K. Yazaki, Nucl. Phys. A436, 593 (1985).
13. F. Gross and D. O. Riska, Phys. Rev. C36, 1928 (1987);
W. Bentz, Nucl. Phys. A446, 678 (1985).
14. J. D. Bjorken and S. D. Drell, Relativistic Quantum Mechanics, (McGraw-Hill, New York, 1964).

15. L. S. Celenza, A. Pantziris, C. M. Shakin, and Hui-wen Wang, Brooklyn College Report: BCCNT 91/021/213 (1991). Submitted for publication in Physical Review C.
16. A. L. Fetter and J. D. Walecka, Quantum Theory of Many - Particle Systems (McGraw - Hill, New York, 1971).
17. A. E. L. Dieperink and P. K. A. deWitt Huberts, Ann. Rev. Nucl. Part. Sci. **40**, 239 (1990).